46TH TURBOMACHINERY & 33RD PUMP SYMPOSIA
HOUSTON, TEXAS | DECEMBER 11-14, 2017
GEORGE R. BROWN CONVENTION CENTER

Optimizing Component Selection in Synchronous Motor Compressor Trains Based On Technical and Financial Considerations

Martin D. Maier
Principal Rotor Dynamic Analysis Engineer
Research and Development Business Unit
Dresser-Rand business, part of Siemens Business Power and Gas
Olean, New York, USA
mmaier@siemens.com

Garry Studley
Process Simulation Engineer
Olean Operations
Dresser-Rand business, part of Siemens Business Power and Gas
Olean, New York, USA
gstudley@siemens.com

Martin D. Maier is a Principal Rotor Dynamic Analysis Engineer at the Dresser-Rand business, part of Siemens Power and Gas. He has 40 years of experience with Dresser-Rand in torsional and lateral rotor dynamic analysis, coupling, bearing and seal design, and machinery vibration analysis as it relates to product development and production support. His experience includes program automation, engineering standards development and vibration troubleshooting. Mr. Maier received a B.S. degree in Physics in 1977 and a B.S degree in Mechanical Engineering in 1990, both from the Rochester Institute of Technology. He is a licensed Professional Engineer in New York State, since 1991, and is a member of the Vibration Institute with a Level IV, Machinery Analyst Certification. He has received a number of U.S. patents in bearing, seal and aerodynamic design.

Garry Studley is a Process Simulation Engineer at the Dresser-Rand business, part of Siemens Power and Gas. He has nine years of experience with Dresser-Rand as a Product Design Engineer, Project/Packaging Engineer and his current position in Process Simulation. Garry graduated from the Rochester Institute of Technology in 2008 with a B.S. degree in Mechanical Engineering and a Masters of Engineering.

ABSTRACT

Compressor trains driven by constant speed synchronous motors need to be designed to withstand high levels of oscillating torque during transient startup conditions when motors are started across-line. The importance of accurately predicting peak torque levels at resonance is critical for component selection to produce a technically acceptable design in the most cost effective manner. This process consists of three phases - (1) a preliminary torsional vibration evaluation performed in the proposal development phase based on available data using a simplified calculation method; (2) a traditional train torsional vibration analysis performed in the production phase when more detailed information becomes available based on a fixed value of assumed modal damping; and (3) a special coupled torsional-lateral analysis which provides more accurate results for geared systems. This procedure is illustrated using a 6 MW, 4-pole, synchronous motor train as an example where the peak torques during startup were found to approach 10.2 Per Unit Torque throughout the shaft line. Numerous means were investigated to reduce the peak torques and associated stress levels which include the following: (1) increase the size of all major train components; (2) step down transformer to reduce the terminal voltage and corresponding motor air gap torques; (3) elastomeric coupling; (4) grid style coupling; (5) slip clutch coupling; (6) viscous rotational damper; (7) hydraulic clutch to disengage the driven components during startup; (8) pony motor plus hydraulic clutch to soft start the train; (9) VFD starter; (10) reducing compressor load torque; (11) custom motor with more favorable startup torque characteristics. The benefits and tradeoffs of each option are evaluated from both financial and technical perspectives. All cost data presented in this paper have been normalized to the base cost of the major bought-out equipment determined at the proposal stage (i.e. base cost = motor + gear + couplings = 1.0). The results of the preliminary evaluation, traditional torsional analysis, and special coupled torsional-lateral analysis are compared and discussed in detail. The coupled analysis, though more complex, provides more precise startup torque levels and often show higher levels of system damping compared with the traditional torsional analysis. The effects of gear bearing design and system parameters on the effective system damping are quantified from the coupled analysis for the subject example for two gear bearing sizes. The cost evaluation presented in this paper applies to the cited example only and is intended to demonstrate the selection process recognizing that other applications may produce different results.

INTRODUCTION

High levels of torsional vibration are experienced during direct-on-line starts of synchronous motor trains which need to be thoroughly evaluated to ensure a reliable design. Twice-slip frequency (2 x sf) pulsating torque is generated at the motor airgap during startup due to the saliency (i.e. non-uniformity) of the motor rotor. This excites the torsional natural frequencies between twice electrical supply frequency and the static condition as the rotor accelerates to synchronous speed. The magnification of the system response depends on the deceleration rate of the motor twice slip air gap frequency and the torsional damping present in the system. API 617, eighth edition, section 2.8.7.5 requires that motor driven trains be designed for the startup condition as well as steady state operation to avoid resonance with one and two times rotational speed(s) and electrical frequencies. Electrical fault analyses are also performed depending on the application requirement.

The design considerations relating to the motor startup characteristics herein described deals exclusively with constant speed synchronous motors started across-line. Induction motors do not demonstrate high peak torque characteristics during startup largely due to their more symmetric rotor design. Induction motors are typically less expensive than synchronous motors but the operational cost is higher due to the lower power factor (typically 0.75 to 0.90) where the utility cost is based on apparent power rather than the actual power. As synchronous motors typically possess a unity power factor, the operational cost is lower as the utility cost is based on actual power consumed. For this reason, induction motors are typically selected for low power applications while synchronous motors are typically selected for high power applications. For intermediate power levels, it is a judgment call based on the tradeoff between up-front purchase price and long term operational cost.

For synchronous motors, there are two major types of rotor construction: laminated pole and solid pole. Laminated pole motors generate lower levels of pulsating air gap torque than solid pole motors which results in lower startup torques and associated stress levels. However, laminated pole motors are subject to mechanical stress limitations which limit them to low speed applications (6-pole @ 1,200 RPM for 60 Hz supply). The trend in industry is to select less expensive motors that operate at higher speeds (4-pole @ 1,800 RPM and 2-pole @ 3,600 RPM for 60 Hz supply current). Often times, the lower motor cost for solid pole motors is offset by higher costs for the driven equipment (gear, couplings, etc.) necessary to transmit the higher startup torques.

In a startup simulation for synchronous motors, four main aspects of the mechanical design need to be evaluated:

- The peak torque capacity of the couplings; more specifically, the torque capacity of the flexible elements which represent the coupling's weak link.
- The torque capacity of the shaft-to-hub juncture (integral flange, hydraulic fit, keyed fit,etc.)
- The fatigue life of the shafting; both the shaft diameter and stress concentration need to be considered to determine the weak link locations along the shaft line.
- Gear teeth contact stresses

API 671 requires a minimum peak torque service factor of 1.15 relative to the coupling peak torque rating and the shaft-to-hub juncture. A fatigue analysis is usually required to determine the number of allowable starts.

For synchronous motors started across-line, keyed shaft ends are usually avoided due to fatigue considerations. Hydraulic fit shaft ends are frequently limited by slip capacity. Integral flanged shaft ends are best suited for the motor and gear shafts as they provide adequate torque capacity with minimal fatigue concerns. Particular attention needs to be paid to the size and positioning tolerances of the flange bolt holes to ensure uniform load sharing by the bolts. Ideally, bolted joints should be designed to transmit torque through flange friction rather than through the bolts in shear but this is not always possible.

The following options are available to the designer to reduce the peak startup torques and associated stress levels in synchronous motor trains:

- Reduce pulsating motor air gap torque by modifying the motor electrical parameters
- Reduce air gap excitation by reducing terminal voltage
- Reduce startup load by activating the surge control (recycle) valve, suction throttling, etc.
- Increase system damping
- Increase shaft diameters and reduce stress concentrations to reduce localized stress levels
- Increase material strength
- Adjust system parameters (inertias and torsional stiffnesses)

Motor startup curves are provided by the motor supplier typically for infinite bus (100 percent terminal voltage) and reduced voltage (typically 80 percent terminal voltage). The mean and pulsating air gap torques and load torque are normalized relative to the rated motor torque and expressed in terms of 'Per Unit' torque or P.U. New installations generally possess strong electrical grids and experience voltage dips less than 10 percent. Old installations which are often encountered with field upgrades and revamps frequently have weak electrical grids where voltage dips can be as high as 30 percent. To validate assumptions relative to electrical grid strength and load for existing equipment, the terminal voltage, speed and gearbox vibration should be recorded as a function of time during startup. Nevertheless, it is prudent to design the system to withstand startup torques based on infinite bus as worst case as the electrical grid could be upgraded in the future or existing equipment on the same electrical supply could be removed from service.

A synchronous motor's electrical design is dictated by API 546 "Brushless Synchronous Machines-500 KVA and Larger", Third Edition, standards. Design guidelines that influence motor startup characteristics include the following:

- Section 2.2.4.1 states that the motor should be able to start at 80 percent terminal voltage. As air gap torque varies with voltage-squared, the air gap torque is reduced to a factor of (0.80)^2 or 64 percent.

- Section 2.2.4.3 states that a 10 percent margin needs to be maintained between the mean motor torque and load torque for all speeds between zero and synchronous speed.

- Section 2.2.6.1.a states that the locked rotor (inrush) current should not exceed 500 percent of the full load current.

Thus, if the train load torque (inclusive of the compressor power, gear power loss and dissipative power at all bearings, windage, etc.) at the point where the load torque curve is at closest proximity with the mean torque curve is, say, 0.58 P.U., then the mean motor torque needs to be at least 0.58/(0.80)^2/0.90 = 1.0 P.U. at this condition to satisfy these requirements.

A higher load torque necessitates increasing the mean torque. The electrical design of the motor is such that the pulsating torque and mean torque vary in a similar manner. Thus, a high load potentially increases both the mean torque and pulsating torque which reduces the acceleration rate at resonance thereby increasing the magnification factor 'Q'. All three considerations increase peak torque levels along the shaft line during startup.

The average and pulsating motor air gap torque and load torque are of primary interest at the instant when the twice slip frequency momentarily coincides with the predominant torsional natural frequency. The predominant torsional natural frequency is the one which produces the greatest system response from motor induced excitation. The predominant torsional natural frequency for single ended motors is the first (fundamental) natural frequency whereas the predominant torsional natural frequency for doubled ended motor is typically the second torsional natural frequency.

The speed at which resonance occurs is given from the following expression:

$$N = Rated\ Speed * \left(1 - \frac{Torsional\ Natural\ Frequency\ [Hz]}{2 * Electrical\ Frequency\ [Hz]}\right)$$

In single ended motor trains, resonance with the first torsional natural frequency typically occurs at 80 percent to 92 percent synchronous speed for 60 Hz electrical supply and 65 percent to 78 percent synchronous speed for 50 Hz electrical supply, regardless of pole number.

With regard to shaft stress evaluations, there are many fatigue life prediction methods used throughout the industry. They are divided into two main categories: stress-based and strain-based methods. Stress-based methods are typically used when the calculated strain is primarily elastic which occurs for life predictions greater than 50,000 starts. Strain-based methods are typically used when the calculated strain is largely plastic which is the case for life predictions less than 5,000 starts. The traditional stress-based 'S-N' method uses the ultimate tensile strength to determine a material's ability to withstand cyclic stresses. The strain-based methods evaluate both the elastic and plastic components of strain which considers both the material's strength and beneficial influence of the material's ductility. Strain-based methods are generally considered more precise and provide more favorable fatigue life predictions than traditional stress-based methods.

One of the main parameters that influence peak torque levels at resonance is the system damping which is typically expressed as modal damping either as a damping ratio (i.e. 0.02) or percentage of critical damping (i.e. 2 percent) . Corbo (2002) reports that for geared systems, damping ratios ranging from 0.02 to 0.05 are commonly used in the industry. This is based on work published by Chen (1983), Anwar and Colsher (1979), Mruk (1978), Write (1975). The reason for this variation relates largely to damping contributed by coupled torsional-lateral damping in parallel axis gearboxes. Torsional damping in a gearbox is produced by three main sources:

- Lateral motion which occurs within the bearing oil films due to the coupling of the torsional-lateral degrees of freedom at the gear mesh. More specifically, the torque that is transmitted across the gear mesh gives rise to lateral gear loads. This torque has both steady and alternating components. The resulting lateral motion within the gearbox bearings dissipates energy which is torsionally induced. In this respect, the bearing design of the gear has a direct influence on the magnitude of torsional damping.

- Gear backlash which occurs when the alternating torque exceeds the mean torque as the gear teeth move in and out of mesh. The impact load at the points of tooth contact as well as the squeeze film action that occurs when the oil is squeezed out of the cavity formed by adjoining teeth dissipates energy.

- Non-linearities associated with the gear backlash change the system dynamics as the teeth repeatedly engage and disengage. Highly non-linear systems do not display a discrete natural frequency and exhibit what is commonly considered a form of 'pseudo-damping' although energy is not dissipated, in the classic sense.

To better quantify the amount of damping present in the system during quasi-resonance conditions, a coupled torsional-lateral analysis can be performed. In such instances, the bearing characteristics of the gearbox need to be known and a program capable of modeling torsional-lateral coupled systems is required. Pradetto and Baumann (2015) presented the results of coupled torsional-lateral analyses of three geared trains and found that the effective damping ratios, as determined by field testing, ranged from 0.032 to 0.065 which were substantially greater than the 0.025 ratio commonly used in the industry. The contribution to overall system damping from the gearbox bearing characteristics as a function of load were discussed, as well as the contribution from mode shape as influenced by the system parameters (inertia and torsional stiffness) were discussed by the authors. Adjusting the system parameters changed the mode shape and shifted the resonance condition to a speed where the motor torques and load torque produced a lower system response.

A simple calculation method is included in Appendix 1 which is a closed form solution for a multiple degree of freedom system based on the assumption that all of the torsional deflection occurs between the motor and gear and that the gear and compressor(s) oscillate in unison. This is generally valid for common systems. Empirical constants 'Alpha', 'Beta', and 'Gamma' are used to account for deviation from this assumption arising from relative deflection elsewhere in the train. Typical values for 'Alpha' range from 0.85 to 1.05. Typical values for 'Beta' and 'Gamma' range from 0.95 to 1.15.

Figure A-1 contained in Appendix 1 gives the dynamic magnifier (Q-Factor) as a function of both system damping and acceleration rate of the twice slip frequency relative to the first torsional natural frequency. The acceleration rate is a function of the following parameters:

- Motor mean torque
- Load torque
- Total train inertia

The load torque during startup is application specific. If it is not known, then for compressor trains, it can be approximated based on the fan law, speed squared, relationship. As resonance with the first torsional natural frequency typically occurs at 85 percent rated speed for 60 Hz electrical supply, the load torque at resonance would be approximately (0.85)^2 = 0.72 rated compressor torque. This is a highly pessimistic estimate as compressors are typically unloaded by suction throttling or starting with the recycle (surge control) valve fully open. This gives conservative results as a higher compressor load will reduce the acceleration rate through resonance yielding a higher, less favorable, value for the dynamic magnifier 'Q'. As shown in Appendix 1, the acceleration rate of the twice slip frequency relative to the first torsional natural frequency is defined as 'q' which is used to determine magnification factor 'Q' from Figure A-1.

There are two noteworthy limiting cases shown in this figure. The first is the case of zero damping where Q = 3.67*SQRT(q) which can be used to provide a worst case estimate for rapid acceleration rates. The second is the case for steady state conditions where Q = 1/(2* damping ratio) which can be used as a worst case estimate for slow acceleration rates. It can also be used for highly damped systems where magnification factor is less influenced by acceleration rate.

An illustrative example shown in Figure 1 is representative of a typical single body compressor train which shows the influence of inertia distribution on shaft torque. In this example, the motor comprises 33.3 percent of the total train inertia and load inertia comprises 66.7 percent of the total train inertia distributed to the gear and compressor by varying amounts. Typical motor startup characteristics are assumed for Mean Torque (1.10 P.U.), Pulsating Torque (0.65 P.U.) and Load Torque (0.35 P.U.) at resonance. The left portion of the curve is representative of trains that involve low speed, low gear ratio (GR~2), large frame size compressors. The

right portion of the curve is representative of trains that involve high speed, high gear ratio (GR~9), small frame size compressors.

The following trends are noted:

1. For trains with a relatively low gear inertia, the shaft torque between the motor and gear is 7.5 P.U. while the shaft torque between the gear and compressor is 7.5 p.u. indicating little attenuation across the gear mesh. Note that 1 p.u. (high speed) = 1 P.U. (low speed) / gear ratio, where 1 P.U. references rated motor torque.

2. The shaft torque between the motor and gear is constant based the assumption that all of the torsional deflection occurs between the motor and gear. In reality, shaft deflection will occur, in some measure, elsewhere in the train causing the peak torque at the low speed end to trend downward with decreasing gear inertia ratio.

3. The shaft torque between the gear and compressor varies from approximately 7.5 p.u. to 1.0 p.u. depending on the inertia distribution.

4. For a uniform inertia distribution (i.e. motor: 33.3 percent; gear: 33.3 percent; compressor: 33.3 percent), the shaft torques are 7.5 P.U. between the motor and gear and 4.0 p.u. between the gear and compressor.

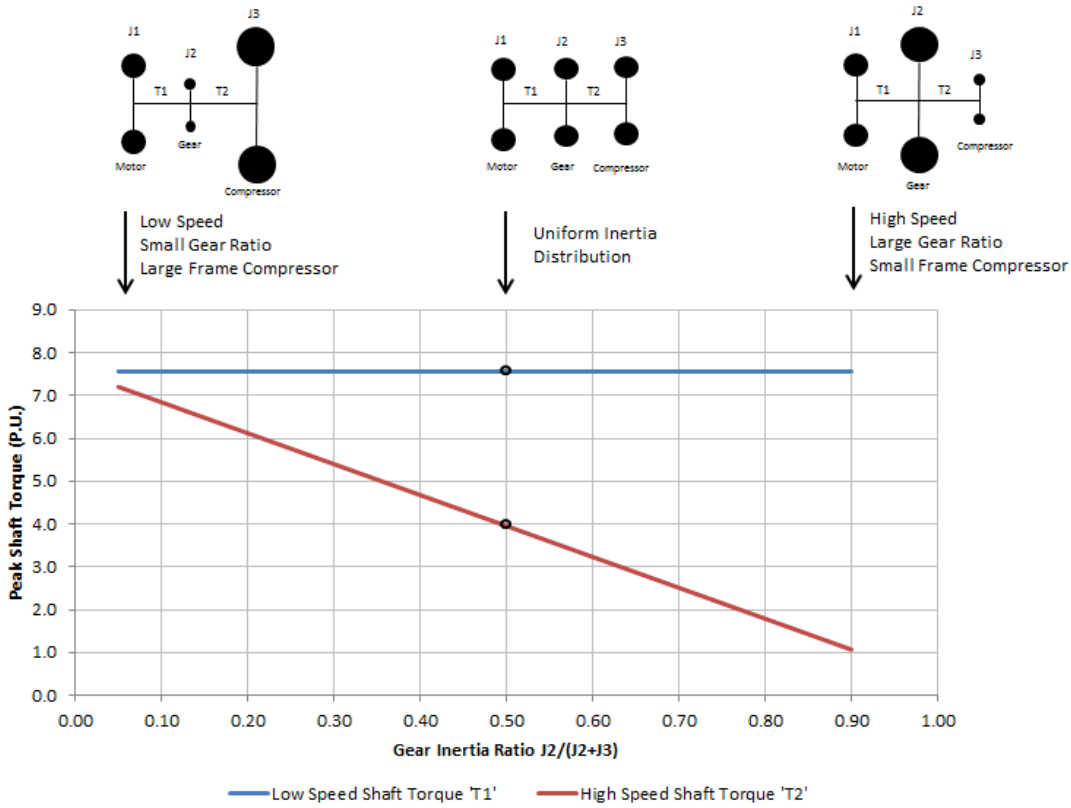

Figure 1- Illustrative Example of the Peak Startup Torques in a Typical Single Body Compressor Train

This example clearly shows that the peak torque levels on the high speed end are a strong function of inertia distribution. This demonstrates that the common practice of using service factors to size shaft ends, couplings and gear meshes for all train arrangements is wholly inadequate. Inertia distribution and startup load needs to be considered as well. For this example, using a service factor for

the high speed shaft based on a peak transient torque of, say, 4.0 P.U. will result in oversizing the couplings in some instances and undersizing the couplings in other instances. Oversized couplings increase cost, negatively impact the lateral rotordynamics of the driven equipment, promotes interference conditions with casing and piping, and increase windage and associated coupling guard temperature. Undersized couplings and shaft ends, when discovered late in the production phase, seriously impact the production schedule and results in cost overruns associated with scrap charges and expedited delivery charges for both the coupling(s) and shaft forgings.

The sizing of train components in synchronous motor trains is often times an iterative process. Initially, service factors may be applied to the rated motor torque to size the couplings, shaft ends and hub-to-shaft interfaces; however, a torsional evaluation is subsequently necessary to make whatever adjustments are needed to comply with industry standards.

The simple closed form solution contained in Appendix 1 can easily be coded into a spreadsheet program such as MS Excel. A more precise method for determining peak torque levels is contained in Appendix 3 which is based on a normal mode synthesis approach. This method is commonly described in vibration texts. This is more complicated than the method used in this study but can be coded into a solver such as MATLAB.

To illustrate the method herein described, a case study is presented below which exhibited unusually high peak torque levels during startup and warranted a thorough investigation of available options to provide the best solution from both technical and commercial perspectives.

BACKGROUND

The compressor train which is the subject of this study and illustrates the selection process is shown in Figure 2. It is a single body compressor train for Alkylation Refrigeration Service with the entire train arrangement and the dry gas seal system set on a common baseplate. The driver is a 6 MW, 4-pole, constant speed synchronous motor driving through a double helical gearbox with a gear ratio of 2.107, to a straight-through, centrifugal, barrel type compressor. The centerline-to-centerline distance of the original gearbox was 16 inches but was later increased to a larger frame size with a centerline-to-centerline distance of 22 inches. The compressor inlet pressure is near atmospheric with an inlet capacity of 36,000 ACFM.

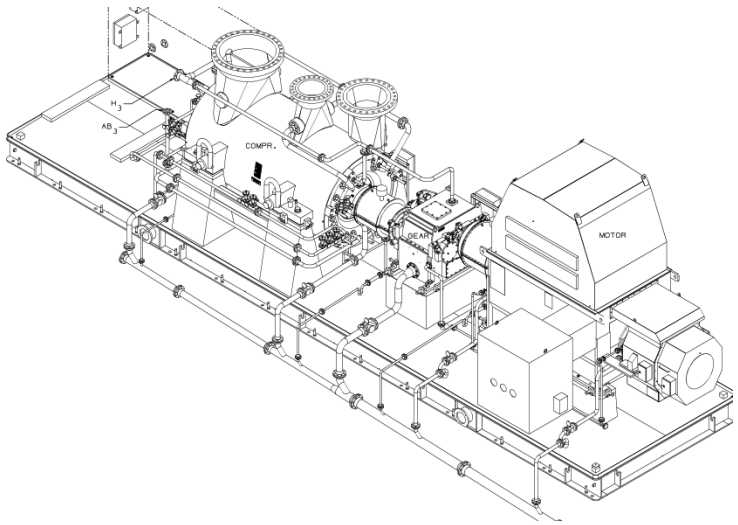

Figure 2 – Train Arrangement

The customer specified additional requirements over and above API standards:

- The closed loop design did not allow the case pressure to be reduced following shutdown by venting or flaring the gas due to environmental considerations. This resulted in relatively high startup loads. The settleout pressure and associated startup load characteristic was determined pre-quote with a dynamic simulation study. This high load was particularly challenging to the motor supplier from an electrical design standpoint.
- Limited physical floor space to fit within the prescribed footprint.
- A simple train arrangement with nothing superfluous added.
- Budgetary constraints which did not allow for cost overruns.
- As this is for a refinery/petrochemical application, the minimum required number of starts was 10 starts per year. This is in contrast to 20 starts per year typically specified for other land based applications.
- The couplings needed to be a single diaphragm design with a preference for a supplier with long lead times.
- Spare couplings, bearings and dry gas seals were required.

In the pre-quotation phase, the respective OEM's used fixed service factors to size the couplings, shaft ends and related components. It was subsequently determined that the shaft line possessed insufficient torque capacity prompting the need to consider other options to reduce peak startup torque.

Figure 3 is a motor startup curve for the original motor which shows curves for the average motor torque, twice slip pulsating motor torque and compressor load torque plotted as a function of speed. These torques are normalized relative to rated motor torque (1 P.U.). Curves are shown for 100 percent terminal voltage (infinite bus) and 90 percent terminal voltage.

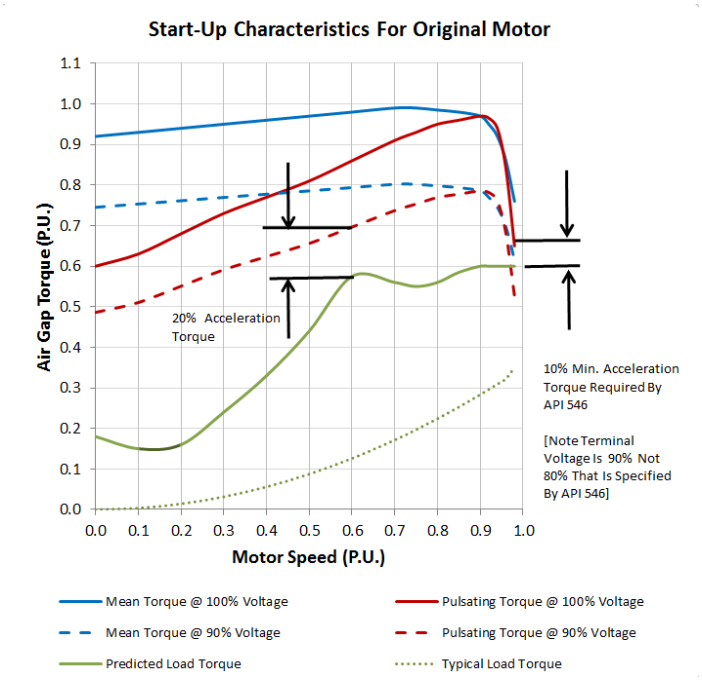

Figure 3 – Startup Curve For Original Motor

Resonance with the first torsional natural frequency during startup occurs at 84 percent synchronous speed. The compressor load at this point in time is 0.58 P.U. motor torque. The electrical parameters of the motor were selected to produce the required torque level in an attempt to comply with API requirements. The point of closest proximity between the mean motor torque and load occurs at 60 percent and at 97 percent speeds. Although API 546, section 2.2.4.1 and 2.2.4.3 requires a minimum separation of 10 percent at 80 percent voltage, this requirement is satisfied only at 90 percent terminal voltage. The customer accepted this deviation from API as the electrical grid was considered quite stiff and the current draw for the relatively small motor will not result in a substantial drop in terminal voltage. It should be noted that both the load torque and pulsating air gap torque are approximately 1.5 times higher than typical applications. The motor startup torque curve for the final, as manufactured, motor is shown in Figure 4. This is a customized design to address the unusually high startup load. The pulsating motor torque at resonance (84 percent motor speed) is 0.65 P.U. compared with 0.96 P.U. for the original motor. In both instances, the mean torque is consistent with what is considered typical. In addition to the unique motor startup characteristics and load torque, the train inertia distribution is of particular interest where inertia of the compressor comprised 66 percent of the total train inertia. As previously discussed, a high load inertia serves to increase peak startup torque levels, particularly on the high speed end of the train.

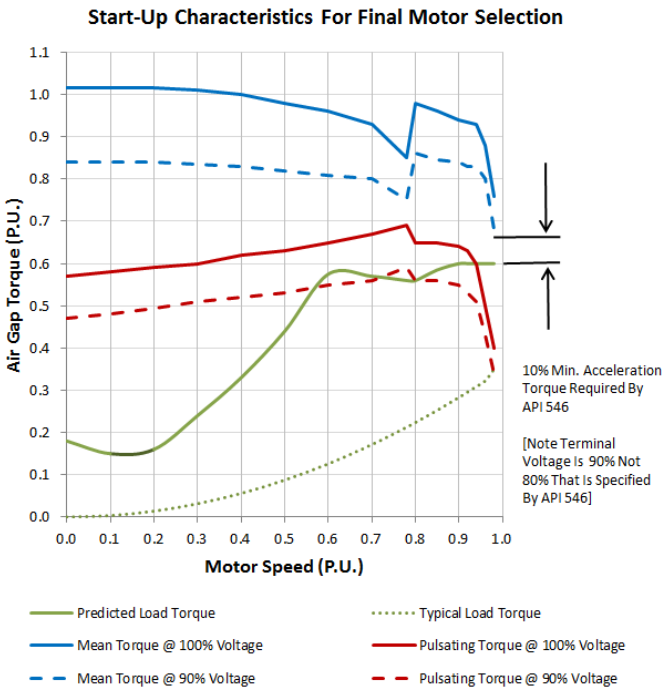

Figure 4 – Startup Curve For Final Motor

The closed form solution previously described was used to determine the peak torque levels at resonance. Appendix 2 contains calculations for the base offering that was initially quoted as well as for alternate train configurations and design options. For the base offering, estimated peak torque levels were found to be 10.2 P.U. and 10.2 p.u. at both the low speed and high speed shafts, respectively. The following observations are made from this calculation:

- The alternating torque is the main torque component at resonance.
- Little attenuation occurs across the gearbox as the gear makes up a relatively small fraction of the total train inertia.
- The high air gap pulsating torque and high load inertia are major contributors to the high alternating torque.
- The elevated magnification factor is the direct result of a slow acceleration rate through resonance due to the relatively large startup load.

It was subsequently determined that all train components, as originally selected, were unable to handle these torque levels including the couplings, shaft end interfaces, gear mesh tooth stresses and fatigue life of all shafts. An initial attempt was made to "beef up" the shaft design until it was learned that the torque levels within the motor rotor exceeded the manufacturer's design limits based on the stated application requirements. Consequently, various design options were considered to reduce the magnitude of the peak torque levels to produce a torsionally acceptable design. The cost impact for each design option is discussed below. Peak torque calculations for each case appear in Appendix 2. Empirical constants 'Alpha', 'Beta' and "Gamma' were back-calculated from full analysis results to demonstrate the range of values. Case 1 involves a larger motor frame size. Cases 2 through 10 involve the original, as-quoted motor. The last option discussed is for the final design (Case 11) involving a customized motor.

Cost data was compiled for 11 different options to provide a solution that was both cost effective and technically acceptable. This cost data was then normalized relative to the base cost of the major bought-out equipment that was determined at the proposal stage (i.e. base cost = motor + gear + couplings = 1.0). These design options are briefly discussed below.

Case 1: Increase Component Sizes

The motor frame size needed to be increased as the torque capacity of one of the motor rotor components was exceeded. The increase in frame size increased the motor inertia from 28 percent to 48 percent of the total train inertia. The pulsating air gap torque at resonance decreased from 0.96 to 0.83 P.U. Both factors resulted in a substantial reduction in peak torque levels. The estimated peak torques on the low and high speed shaft dropped to 7.0 P.U. / 6.5 p.u., respectively. Nevertheless, the gearbox, couplings and shaft end diameters of all train components needed to be increased. The tooth profile of the gear mesh required modification to reduce contract stresses and higher strength material was selected. Increased component sizes increased the size of the train which was unfavorable to the customer as the available footprint was limited. The cost factor associated with the major buyouts was 1.37 relative to the as-quoted, base offering of 1.00.

Case 2: Step Down Transformer to Reduce Terminal Voltage and Motor Air Gap Torque Levels

A step down transformer is used only during startup. Once up to speed, the transformer is switched out of the circuit. A speed squared relationship exists between the motor air gap torque (both mean and pulsating components) and terminal voltage. A transformer can potentially be selected to reduce the terminal voltage down to 80 percent during startup. However, in this instance, a terminal voltage of 90 percent is necessary to accelerate the train to speed to preclude stall. This reduces the motor air gap torques to (0.90)^2 -> 81 percent of the infinite bus values. This effect is offset, in part, by the increased magnification factor at resonance which changes from 14.3 to 16.3 due to the slower acceleration rate through resonance. The net result is that the peak torque levels on the low and high speed shafts reduce to 9.1 P.U. and 9.1 p.u., respectively. The gear and low speed coupling needed to increase by one size increment. The high speed coupling needed to be increased by two size increments. The compressor shaft end diameter, journal bearings and dry gas seals needed to increase to the next standard sizes. The tooth profile of the gear mesh required modification to reduce contact stresses and higher strength material was necessary. In this instance, a step down transformer provides minimal benefit due to the high startup load which limits the voltage reduction. An advantage of a step down transformer is that it reduces the impact of startup on other equipment on the same electrical supply. Disadvantages include possible longer wait times between successive hot (re)starts and increased real estate to accommodate the transformer. The lead time for a transformer is typically 20 to 24 weeks. The cost factor for this option is 2.33.

Case 3: Elastomeric Coupling Between Motor And Gear

Elastomeric couplings (a.k.a. Holset style or rubber block couplings) are frequently used in the industry between the motor and gear for synchronous motor applications to increase system damping. The rubber blocks are typically wedge-shaped or have a cylindrical profile and transmit the torque from hub-to-sleeve in compression. The elastomeric half is usually on the motor side and a conventional flexible element (diaphragm or disk style) is typically on the gear side. For unusually severe applications, a tandem block arrangement may be used without a flexible element. Published magnification factors range from 3.0 to 4.0 for high damping SBR block material, depending on block hardness. The *effective* system damping is determined based on the consideration that relative deflection occurs both within the elastomer blocks (high damping) and the steel components (low damping) elsewhere in the train.

For elastomeric couplings, the *effective* magnification factor is approximately 1.6x to 2.0x the published block magnification factor (i.e. Qeff = 1.7 x 3.0 = 5.1). In this instance, the peak startup torques on the low and high speed ends are reduced to 4.5 P.U. and 4.4 p.u., respectively. This enables the original motor and gear to be used. However, the high speed coupling needed to be increased to the next larger size. The advantage of the elastomeric coupling option is proven reliability as they have been in common use in synchronous motor trains over the last 50 years. They also handle high peak transients associated with electrical faults which make the train design more torsionally robust. Although they are a "tried and true" option, the disadvantage of elastomeric couplings is that they are viewed as high maintenance as the blocks need to be replaced approximately every 5 years. Elastomeric couplings are also temperature sensitive, dimensionally larger, heavier and produce more windage compared to conventional flexible element couplings. The lead time for elastomeric couplings is typically 24 to 28 weeks, depending on size and availability of block material. The cost factor for this option is 0.99 considering that there is a customer requirement for one set of spares.

Case 4: Grid-style Coupling Between Motor and Gear

Grid-style couplings are frequently seen in field upgrades and revamps. They were commonly used in the 1960's and 1970's particularly in electric motor applications. The shaft end separations were typically less than one inch. Torque is transmitted through a circumferential, serpentine, spring element which is interwoven between adjoining slots in the coupling hubs. The early versions required continuous lubrication but have since changed to grease packed lubrication. Damping is provided at the contact interface between the spring element and retainers. Attenuation also results from the spring characteristics of the serpentine spring, which is highly non-linear. The magnification factors typically range from 9 to 11. They are not as favorable as elastomeric couplings but are better than what conventional flexible element couplings provide. As with elastomeric couplings, the magnification factor needs to be adjusted to account for compliance elsewhere in the train. The *effective* magnification factor is approximately 1.0x to 1.5x the published values (i.e. Qeff = 1.0 x 9 = 9.0). In the subject application, the peak torque levels on the low speed and high speed ends are reduced to 6.4 P.U. and 6.8 p.u., respectively. This is based on a single element design although dual element designs are better suited for typical shaft separation distances. The larger frame gearbox was needed and the high speed coupling needed to increase by two standard sizes. Grid-style couplings are compact, require less radial space than elastomeric couplings and can accommodate short shaft end separations. The serpentine spring element can be replaced without removing the hubs. They also have a relatively high peak torque capacity. A disadvantage is that the spring element requires a fresh application of grease at every major turnaround. They are not considered API compliant although they have a long history of satisfactory use. The lead time for grid style couplings is typically 12-16 weeks. The cost factor for this option is 1.04. This considers the customer requirement for spares although it could be argued that spares are necessary only for the spring element, which is the low cost item.

Case 5: Slip Clutch Coupling

Conventional flexible element couplings can be fitted with an additional member that transmits torque through frictional forces between intermediate annular surfaces that are pressed together with a prescribed amount of interference. When the torque limit is exceeded, relative motion occurs between the contact surfaces and the surfaces slip relative to one another. The torque downstream of the slip interface is thereby limited as evidenced by the clipped or shaved peaks seen in the time-torque signatures. Slip clutch couplings are typically applied on the low speed end, but in some instances can be used at the high speed end. A good discussion of slip clutch coupling applications is provided by Hutton (2014). If a higher than expected torque overload were to occur, the contact surfaces disengage and the driven component drops onto a bushing or rolling element bearing until the train comes to rest. During a slip event, energy is dissipated at the contact surface which translates into (coulomb) damping. Vibration is also attenuated due to the highly non-linear nature of the device whereby the dynamics of the system momentarily changes following each slip event. As the system is highly non-linear, the simple closed form solution used in the present study is not recommended. However, to establish a frame of reference relative to the other options evaluated in this study, the effective dynamic magnifier which was back-calculated from the clipped torque levels provided by the couplings manufacturer was found to be 4.4. In this application, the peak torque levels with the slip coupling at the low and high speed ends are 3.8 P.U. and 3.6 p.u., respectively which allowed the use of the original motor, gear and couplings. The compressor, bearings and seals could also be reduced in size. The advantage of slip couplings is that the torque limit is adjustable based on the hydraulic pressure used to activate the device. Additionally, the slip element can be reused and reactivated following a major torque overload. One disadvantage is that the design is considered proprietary and the slip characteristics are not generally known and are difficult to analyze with conventional rotor dynamic codes. The lead time for slip clutch couplings is typically 22-26 weeks. The cost factor for this option is 1.02. This considers the customer requirement for spares.

Case 6: Viscous Rotational Damper

A new device recently introduced to the API industry is a torsional damper which imparts viscous damping to the torsional system. It is a drop-in replacement for a spacer in a conventional flexible element coupling and requires no special consideration with regard to operation or maintenance as it is a hermetically sealed assembly. The magnification factor of the viscous rotation damper is approximately 3.0 to 3.5 which is comparable to that of an elastomeric coupling. In the subject case study, the device reduced the peak torque levels on the low and high speed ends to 3.1 P.U. and 2.9 p.u., respectively. Consequently, the originally quoted bought out components were found to be satisfactory from a torque transmission and fatigue life perspective. Moreover, the lower peak torque levels at the compressor allowed not only the shaft end diameter to be reduced but also the journal bearing and dry gas seal to be reduced as the shaft end diameter, in this instance, dictates bearing and seal sizes. This results in a cost reduction which helps to offset the cost of the torsional damper. The disadvantage of this device is its lack of experience in API industry although versions of it have been in widespread use in low speed reciprocating equipment. The lead time for a viscous rotational damper (spool piece portion) is 10-12 weeks. The cost factor is 0.94. This considers the customer requirement for spares.

Case 7: Hydraulic Clutch Preceding Gearbox

A hydraulic clutch, torque converter or fluid coupling can be positioned at the input shaft of the gear which uncouples the driven components from the driver during startup. Once up to speed, hydraulic fluid is introduced into the device which slowly accelerates the driven equipment up to speed. Some varieties contain oil during startup but disengage the driven components through various means. In this way, the only component that is connected to the driver during startup is the low speed coupling and ½ clutch. As the driven inertia is reduced by an order of magnitude, the peak startup torque on the low speed end is reduced to very low levels. The electrical design of the motor becomes much simpler particularly for high startup loads as a large margin now exists between the mean motor torque and the load torque, which is minimal during startup. This may result in a lower cost motor design. The high speed coupling sees no peak torque during startup in this scenario. Once the clutch is filled with fluid and brings the driven equipment up to speed, an optional locking mechanism engages across the hydraulic clutch which precludes relative motion. For the subject application, the original component sizes could be used. Although the peak torque levels on the motor shaft are low (0.4 P.U. on this instance), a steady state calculation is recommended during the early production phase as the first torsional natural speed for this portion of the train during startup can be in proximity with electrical supply frequency which can be excited by current inrush. It is a good design practice to maintain a 20 percent separation margin between the first torsional natural frequency of the low speed branch (i.e. motor + ½ clutch) and electrical supply frequency by adjusting the torsional spring rate of the low speed coupling. Hydraulic clutches are frequently integrated into the gearbox case requiring little additional real estate. Variable speed operation can also be provided over a designated speed range although heat dissipation and associated lube oil requirements increase substantially. The lube oil reservoir is frequently located under the gearbox. Be aware that the cost of the oil system is considerable and is often not included in the quoted cost of the clutch/gear. In the subject application, there is potential to downsize the compressor shaft end, bearings and dry gas seals which result in a cost savings that serves, in some measure, to offset the cost of the clutch. The lead time for an integrated hydraulic clutch & gearbox is typically 26 to 32 weeks. The cost factor is 1.95.

Case 8: Pony Motor + Hydraulic Clutch Preceding Gearbox

This is an adaptation of the previous case (7) consisting of the addition of a small fixed speed induction motor (a.k.a helper or ‘pony’ motor) to the free end of the primary motor which accelerates the primary motor up to speed while the driven equipment is uncoupled from the train. Once up to speed, the windings of the primary motor are energized and the pony motor disengages from the train. As the twice slip excitation is no longer present in the primary motor air gap, this eliminates the peak startup torques that would otherwise occur during startup. As a result, for the subject application, the original component sizes could be used with the potential to downsize the compressor shaft end, journal bearings and dry gas seals. The pony motor is sized to accelerate the primary motor and ½ clutch up to 97 percent rated speed within the time dictated by the thermal limits of the pony motor stator windings (typically 10 percent-20 percent of the rated power level of the primary motor). This method greatly reduces the impact on the electrical grid during startup, which is a particular concern when the current draw is high for high power applications. The disadvantage of this arrangement is that it increases footprint size and adds cost. The lead time for a pony motor is typically 18-22 weeks, depending on size. The cost factor for this option is 2.28.

Case 9: Variable Frequency Drive (VFD) Starter

VFD starters are used to 'soft start' motors to eliminate the high transient torque levels. The VFD starters are sized such that they can provide the necessary torque to overcome the driven load during startup. Once up to speed, they are switched out of the circuit and the motor now operates on electrical supply current (60 Hz or 50 Hz). As the power level is usually less than what conventional VFD drives require during steady-state operation, the excitation levels of the integer and non-integer harmonics during startup are relatively small and do not effect hardware selection. As the power level is a fraction of the rated motor power, the cost is less than a conventional VFD which provides variable speed operation at full load. An added benefit of a VFD starter is that the motor cost may be lower as less copper is required to satisfy the API requirements relative to current inrush at startup. VFD starters, typically LCI drives, can be configured to start multiple trains in an installation in succession. The main disadvantage is that it is an electronic device that has the potential to malfunction which may not be acceptable for critical applications. It also requires physical space to accommodate the electronics module which is a major consideration particularly for offshore use. The lead time for a VFD starter is typically 18 to 24 weeks. The cost factor for this option is 2.60.

Case 10: Compressor Startup Load Reduction

Startup load in compressor trains is directly related to process conditions, specifically, settleout pressure. Settle-out pressure is the case pressure that is attained after the pressurized gas contained between the main suction and discharge valves equalizes following shutdown. It is a design consideration when it is not possible to vent or flare the gas due to environmental concerns. Settleout pressure is a function not only of the pressure differential across the case immediately prior to shut-down but also the volumes of the intake and discharge process piping and valve placement. One method to reduce settleout pressure is to increase the piping volume on the suction side through means of a pressure vessel of a prescribed size. The disadvantage of doing this is cost as well as the additional real estate needed to accommodate the pressure vessel. This option was initially considered for the subject application but was dismissed on the basis of cost. However, the original motor could have been redesigned for lower startup load resulting in more favorable motor air gap torque characteristics. The calculated peak torque levels were 6.2 P.U and 6.2 p.u. on the low speed and high speed ends, respectively. Nevertheless, the size of the gearbox and couplings would need to be increased to handle the elevated torque levels. The cost factor for this option was 1.89.

Case 11: Customized Motor – Final Design

A customized motor design was developed which provides more favorable startup characteristics. The inertia of the new motor was greater (inertia fraction changed from 0.28 to 0.37) and the pulsating air gap torque was reduced from 0.96 P.U. to 0.65 P.U.. Both factors serve to reduce peak torque levels. The peak torque levels at the low-speed and high-speed ends were 6.1 and 5.9 P.U., respectively. The gearbox and couplings needed to be increased to the next standard size. The gearbox bearing diameters likewise increased which altered the lateral dynamic bearing coefficients pertinent to the coupled analysis discussed later in this tutorial. The final design was both commercially viable and technically acceptable based on the application requirements and met with the customer's approval. The cost factor for the final design was 1.14.

Figure 5 is a summary of the cost evaluation study. For this job, there is a customer requirement for spare couplings, bearings and seals so data is presented both with and without spares. The higher cost options shown in this figure are often selected if there is a need to reduce the impact on the electrical grid during startup, particularly for high power applications (P > 20 MW). For a relatively small motor such as this, electrical grid considerations are not significant. For some applications, the need for variable speed operation drives the decision. For the subject application, Case 6 involving the Viscous Rotational Damper was found to be the most cost effective but was perceived to involve higher risk due to its limited experience in the API industry. The other alternate coupling designs that were examined (elastomeric, slip clutch, grid) were found to be cost competitive but were dismissed by the client based on the desire to avoid unnecessary complexities. In the end, Case 11 with the customized motor was viewed as the most favorable choice from the customer's and OEM's perspectives so the decision was made to move forward on that basis.

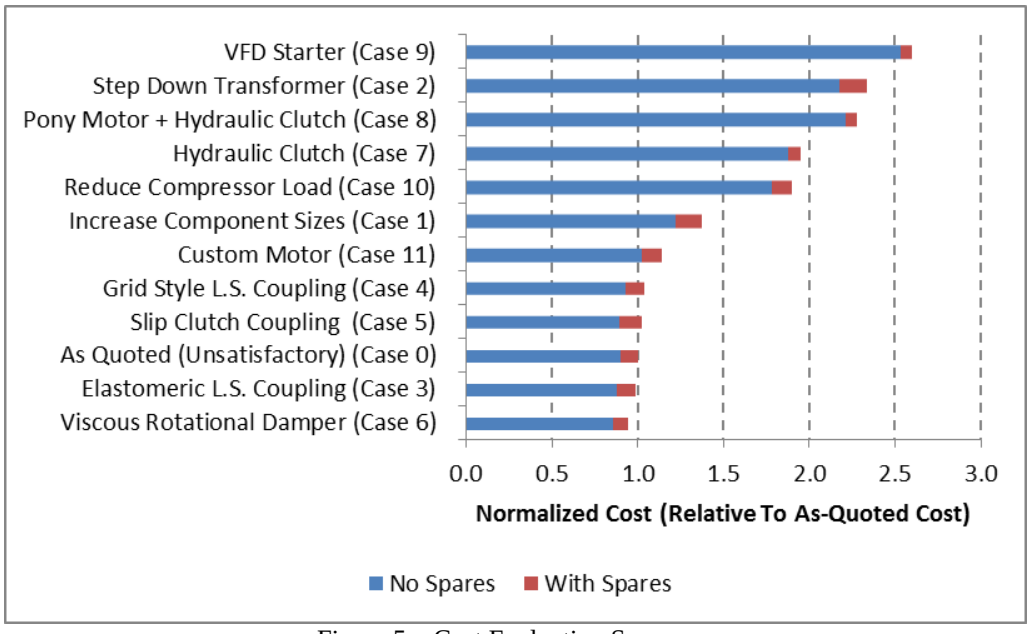

Figure 5 – Cost Evaluation Summary

Standard Torsional Analysis Performed in the Production Phase

Once the final train configuration was determined, a standard transient torsional analysis was performed to confirm component acceptability. The following discussion relates to the final, as manufactured, design.

In the early project phase, little information is generally available for shaft geometry of the major train components. Often time, the opportunity does not exist to wait for the shaft profiles from the major equipment suppliers as decisions need to be made relative to shaft end sizes as it affects coupling selection and shaft forgings. Also, depending on the supplier and the project ship date, the lead time for the couplings requires that the coupling be ordered within the first few weeks after a P.O. is received. Changing shaft end geometry beyond Week Four can result in scrap charges and negatively impact the production schedule. To address this lack of detailed shaft geometry, the torsional stiffness of the shaft ends can be approximated knowing only the journal bearing diameters for each major body. The equivalent torsional stiffness of the shaft ends can be approximated by assuming a length of shaft which is a fixed multiple of journal diameter. For example, a length corresponding to two times the journal diameter provides a good estimate for the shaft end stiffness of the motor, bullgear and pinion shafts. For the drive (non-thrust bearing) end of compressors, a length corresponding to three times the journal diameter provides a good estimate for torsional stiffness. For the driving (thrust bearing) end of compressors in drive-thru applications, a factor of four is appropriate. This approach provides acceptable results in the early production phase. Variations in shaft geometry do not affect the end result significantly considering that most of the compliance of the torsional system is contributed by the couplings, not the shaft ends, particularly if the couplings are a flexible element disk pack or diaphragm styles and the shaft end separation distance is at least 18 inches.

A preliminary model is shown in Figure 6a using this approach. The API data sheets for the motor and gear provide the total rotor inertias. Preliminary coupling data either from proposal drawings or data bases provide the torsional spring rates of the couplings. At this point in the job, only the lower order, coupling dominant, torsional natural frequencies are of primary interest. Figure 6b shows the detailed model used in the final torsional report which was created once the certified vendor drawings became available. The first two modes are tabulated in Figure 6c which were calculated based on the preliminary model and the detailed model. As can be seen, the results differ by less than 1 percent. However, the estimates for major mass inertias could subsequently change during the early stages of a project so separation margins in excess of 10 percent should be maintained, depending upon the estimated accuracy of the data.

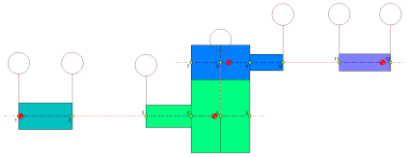

Figure 6a – Preliminary Torsional Model

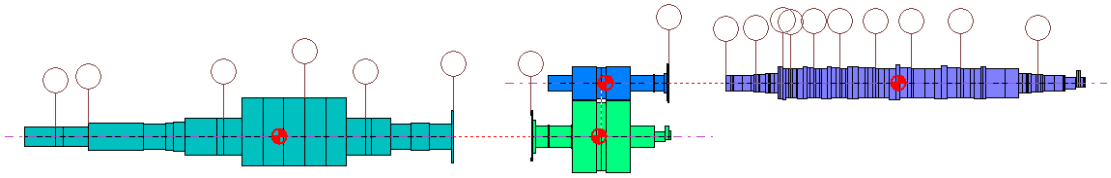

Figure 6b – Final Torsional Model

Mode #	Torsional Natural Frequencies (CPM)		
	Preliminary Model	Final Model	% Difference
1	1,242	1,237	0.4
2	3,200	3,190	0.3

Figure 6c – Comparison of Analysis Results

It should be noted that in geared systems, speed referencing of the system parameters is required, usually performed relative to driver speed. This is accomplished by multiplying the torsional stiffness and inertia values downstream of the gear mesh by the gear ratio squared. Usually, this is done internal to the program prior to computations performed by the solver.

Once geometry becomes available, the final torsional analysis can be pursued. The first step is to determine the torsional natural frequencies and their locations relative to potential mechanical and electrical sources of excitation. This is evaluated on an interference diagram, as shown in Figures 7 and 8. API 617, eighth edition, section 2.8.7.5, requires that a minimum separation margin of 10 percent be maintained with respect to 1x and 2x shaft speeds and 1x and 2x electrical supply frequencies.

Figures 9a and 9b shows the normalized torsional mode shapes for the first two, coupling dominant, torsional natural frequencies. The relative deflections across the couplings and the amplitude at the major components provide the means to qualitatively assess the sensitivity of the natural frequencies on the system parameters. For typical systems, the first torsional natural frequency is a strong function of the low speed coupling stiffness and the second torsional natural frequency is a strong function of the high speed coupling stiffness. The coupling torsional spring rates are adjusted accordingly to achieve proper placement of the torsional natural frequencies.

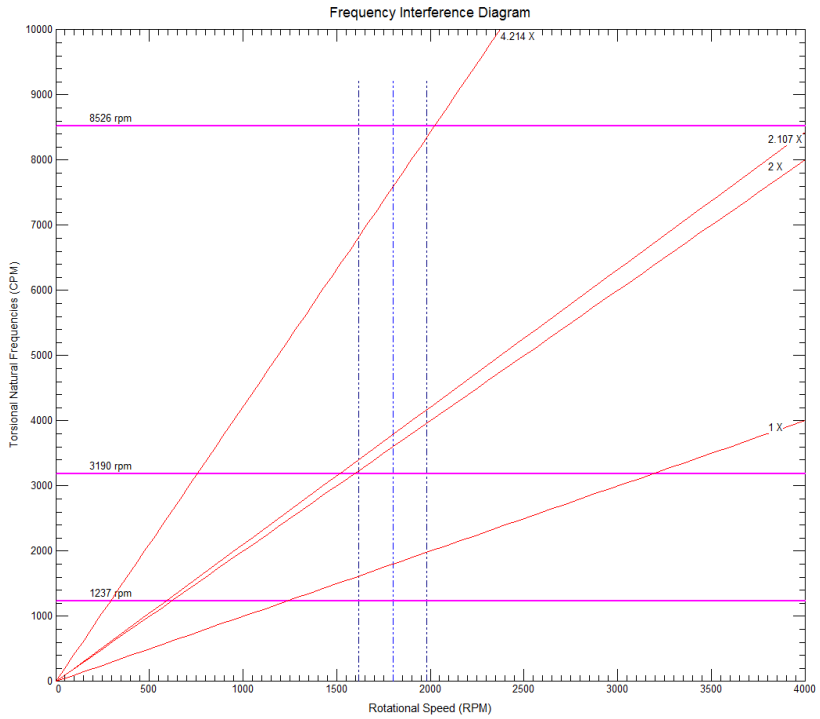

Figure 7 - Interference Diagram Relative To Potential Sources Of Mechanical Excitation (i.e. 1x and 2x shaft speed)

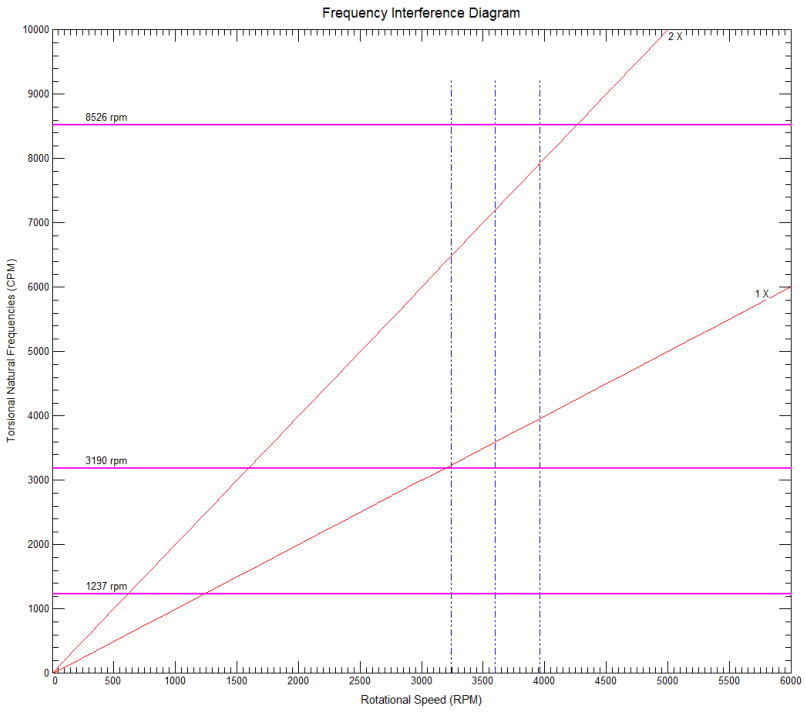

Figure 8 - Interference Diagram Relative To Potential Sources Of Electrical Excitation (i.e. 1x and 2x electrical supply frequency)

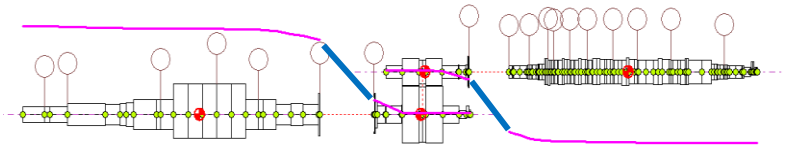

Figure 9a - Mode Shape For First Torsional Natural Frequency (1,237 CPM)

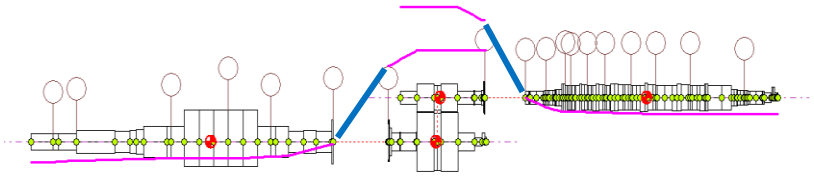

Figure 9b - Mode Shape For Second Torsional Natural Frequency (3,190 CPM)

After the steady state analysis is completed, a transient startup analysis is performed. It is based on the motor torque curve provided by the motor supplier. The infinite bus startup curve for the final, as-built, motor is shown in Figure 4. In the final report, the air gap characteristics were derated slightly to account for a predicted 3 percent voltage dip in the electrical supply. Note the abrupt jump in the mean and pulsating torque at 79 percent synchronous speed. This reflects the custom motor design aspects that needed to be implemented to satisfy the application requirements relative to startup load.

Figure 10 is the plot of motor speed as a function of time. Resonance with the first torsional natural frequency occurs at 13.9 seconds. The torque reversals at resonance are of significant magnitude to produce sizable oscillations in shaft speed as seen from this curve.

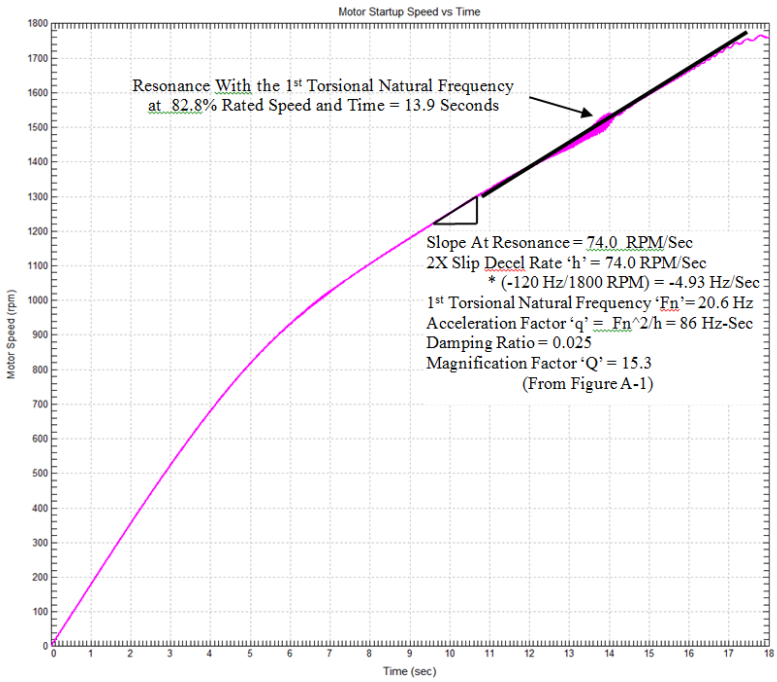

Figure 10 – Train Speed Startup Plot

Figure 11 shows the responses at the low speed and high speed coupling locations when the twice slip frequency component is in momentary resonance with the second and first torsional natural frequencies during startup. The jog in the vertical reference lines occurs because the interference diagram is speed-based, whereas the torque responses are time-based.

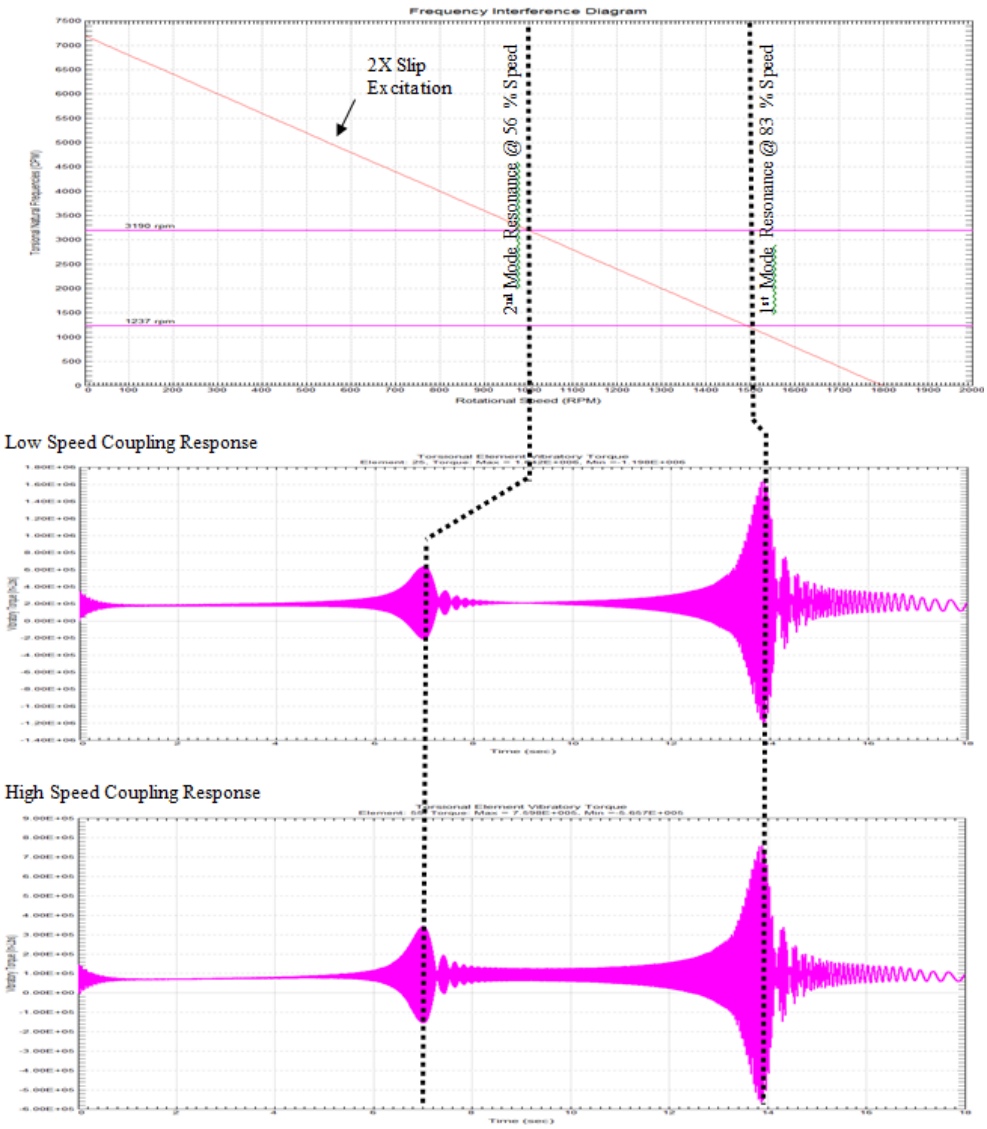

Figure 11 – Coupling Torque Response

Damping is one of the main parameters that influence peak torque levels at resonance. In the torsional analysis, a fixed modal damping of 2.5 percent critical damping was assumed, which is consistent with industry practice. A value of 1.0 percent is attributed to shaft hysteresis damping and 1.5 percent is assumed to be provided by the torsional-lateral interaction within the gearbox. To validate this assumption, a coupled torsional-lateral analysis was subsequently performed.

Special Coupled Torsional-Lateral Analysis

The program used in this study was recently upgraded to handle time transient, coupled torsional-lateral systems; however, at the date of this publication, it did not possess a speed-based startup analysis capability for coupled torsional-lateral systems. This shortcoming was addressed in the current study by using a time-based excitation table which was generated using the acceleration rate that matched the standard torsional startup analysis. It is seen from the startup curve in Figure 9 that the acceleration rate through resonance is fairly constant. A motor acceleration rate of 74 RPM/sec translates into a twice slip frequency deceleration rate of 4.93 Hz/sec. A time-torque tabular listing was then generated using a 'sine swept' equation obtained from Irvine (1998):

Torque (P.U.) = Mean Torque + Pulsating Torque* $SIN\left\{2 * PI * \left[0.5 * \left(\frac{f2-f1}{t2-t1}\right) * t + f1\right] t\right\}$

Where,

- f2 – final frequency
- f1 – initial frequency
- t2 – final time
- t1 – initial time

Since the first torsional natural frequency is of primary interest, a smaller train model was generated to reduce computational time of the coupled analysis. This is shown in Figure 12. The shaft end stiffnesses were fine tuned to match the first and second torsional natural frequencies. The radial bearings for each major train component were modeled for sake of completeness although the influence of bearings for the motor and compressor could probably be ignored as they are far removed from the gear mesh.

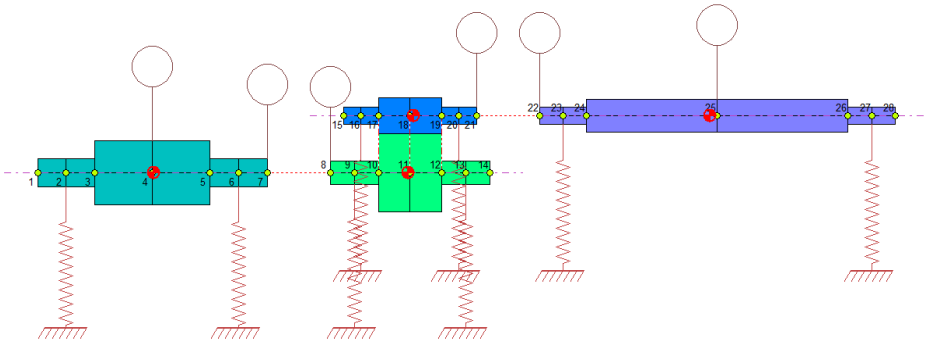

Figure 12 – Coupled Torisonal-Lateral Model

In the coupled analysis, the dynamic coefficients of the bullgear and pinion bearings evaluated at resonance speed need to be included in the model. The big unknown is the effective bearing load used to generate the bearing coefficients recognizing that the bearing coefficients are a function of eccentricity which is related to instantaneous amplitude of vibration. The rotor dynamic code that was used in this study utilizes (fixed) bearing coefficients that are not amplitude dependent. Figure 13 is a sketch of the bullgear and pinion bearings, which in this instance, are ordinary sleeve type, pressure dam, bearings. Key parameters relating to the small bearings in the original gearbox and the large bearings in the final, as manufactured, gearbox are also shown. The pressure angle of the gear mesh is 20 degrees. At resonance, the gear typically undergoes large torque reversals. The bearing film characteristics are highly non-linear as the shafts transverse the range of the full bearing clearance. The manner of modeling bearing loads was discussed in Pradetto (2015). Good correlation with measured field results was reported by assuming a bearing load of 10 percent of rated load. This makes intuitive sense because the dissipation of energy is related to the damping term times the velocity. Since the lateral velocity of the shaft is greatest at low journal eccentricities, the effective bearing damping will be weighted toward the center of the bearing.

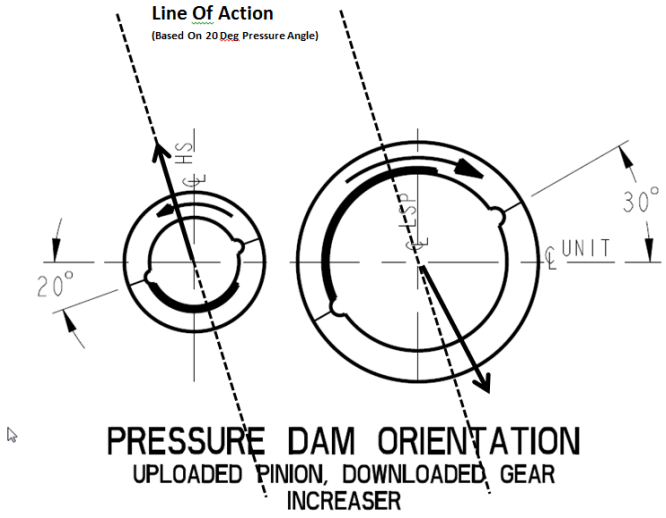

	Original Gearbox w/ Small Bearings	Final Gearbox w/ Large Bearings
Bullgear		
Diameter (In)	7.25	9.25
Length (In)	5.5	5.5
Unit Loading (PSI)	327	187
Surface Speed (Ft/Sec)	57	153
Sommerfeld Number (-)	1.28	2.66
Pinion		
Diameter (In)	5.75	6.75
Length (In)	5.75	6.75
Unit Loading (PSI)	395	209
Surface Speed (Ft/Sec)	95	112
Sommerfeld Number (-)	2.42	4.57
Centerline-To-Centerline Distance (Inches)	16	22

Figure 13 – Gearbox Bearings Load Orientation and Key Parameters

Figures 14 and 15 show the time transient startup torque signatures from the coupled torsional lateral analysis at the low speed and high speed coupling locations. Gear backlash effects were not considered in the analysis as it provides conservative results. These results are comparable to those determined from standard torsional analysis for a fixed value of modal damping of approximately 2.5 percent.

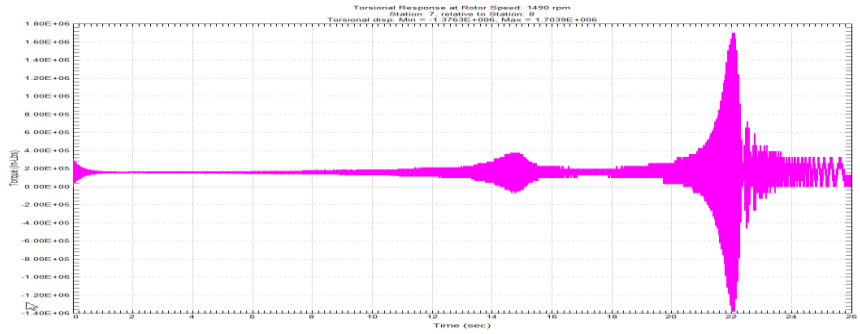

Figure 14 – Coupled Transient Response At Low Speed Coupling

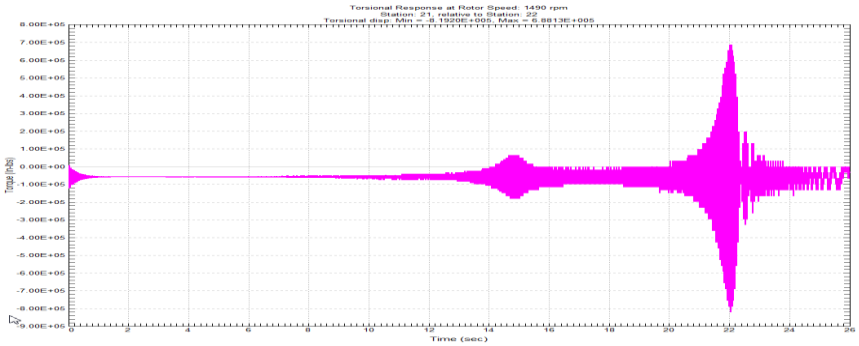

Figure 15 – Coupled Transient Response At High Speed Coupling

Figure 16 shows the calculated steady state response from the coupled torsional lateral analysis at the low speed and high speed coupling locations for the large (final) bearing selection. Curves are shown for three cases which show damping contributed by three separate sources:

1. Shaft hysteresis damping. A value of 1 percent was assumed which is consistent with industry practice.
2. Shaft hysteresis damping plus lateral damping from the bullgear bearings
3. Shaft hysteresis damping plus lateral damping both from the bullgear and pinion bearings

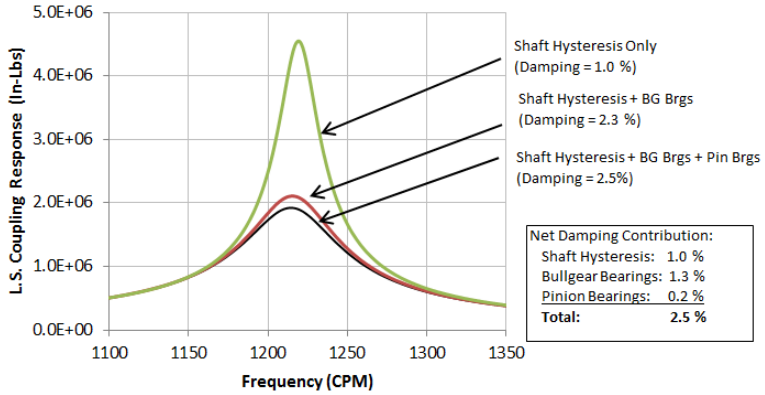

Figure 16 – Coupled Steady State Response at the Low Speed Coupling For Large (Final) Gear Bearings

It is seen from these results that the bullgear bearings contribute the greatest damping (1.3 percent) to the aggregate damping of 2.5 percent. These values were determined using the half power method from the coupled, steady state analysis.

Figure 17 shows a similar plot for the small (initial) bearing selection. For the purposes of this study, the gearbox geometry was kept the same, only the bearing size was changed. It shows a similar trend where the bullgear provides the greatest amount of torsional damping. An unexpected result is that the overall system damping is higher for the smaller bearings than for the larger bearings (3.4 percent vs. 2.5 percent); however, as is observed with lateral rotor dynamics, for a given set of system parameters, there is an optimum damping level that produces the most favorable system response. Although the torque level is lower with the small bearings, the shaft stresses are higher as torsional stress varies with diameter cubed. So in this instance, the large bearing selection results in the lower shaft stresses even though the torque levels are greater.

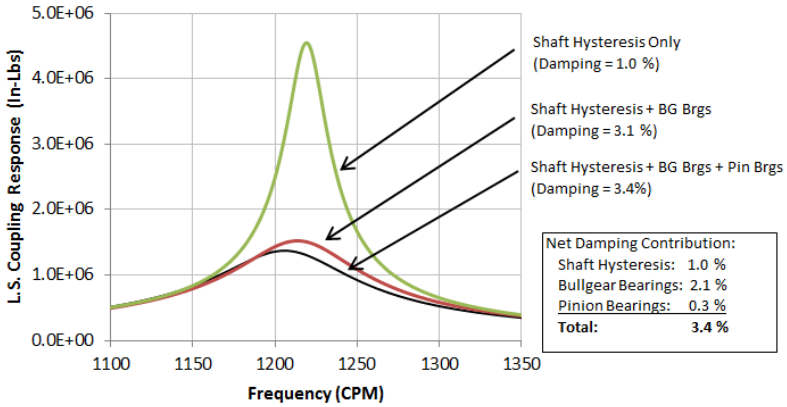

Figure 17 – Coupled Steady State Response at the Low Speed Coupling For Small (Initial) Gear Bearings

A parametric study was performed to determine the effect of coupling (shaft) stiffness on overall damping levels as shown in Figure 18. Coupled response results were generated for a range of coupling stiffness ratios. The coupling stiffness ratio is the ratio between the low speed coupling stiffness and the high speed coupling stiffness relative to driver speed. This is relevant because coupling stiffness is one variable over which the designer has control in the early production phase. The left portion of the plot is for a relatively soft low speed coupling and the right portion of the plot is for a relatively stiff low speed coupling.

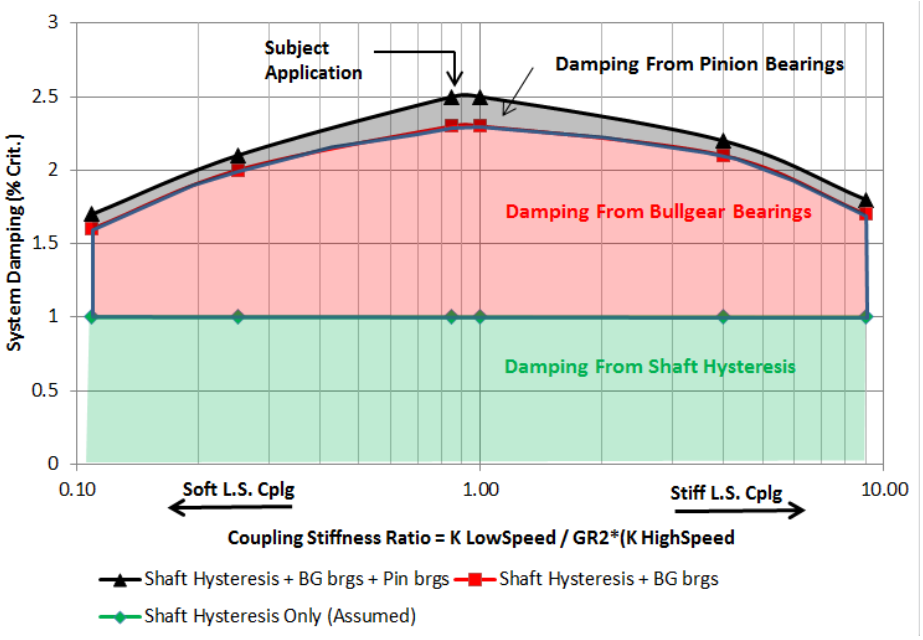

Figure 18 – Coupled Analysis Results Showing Influence Of Shaft Stiffness Distribution On System Damping

Figure 19 shows the mode shapes for both extremes. Please note the location of the nodal points. As one would expect, with a relatively soft low speed coupling, the node is located between the motor and gear. With a relatively stiff low speed coupling, the node is located between the gear and compressor. For the case of equal coupling stiffnesses (while accounting for gear ratio influence), the node is located at the gear mesh. In this particular instance, it seems that positioning the node point at the gear mesh results in the most favorable value of system damping. The subject application is near the optimum value of modal damping of 2.5 percent. Further investigation is required before drawing any general conclusions relative to other train arrangements.

Coupling Stiffness Ratio = .11 (Soft Low Speed Coupling / Stiff High Speed Coupling)

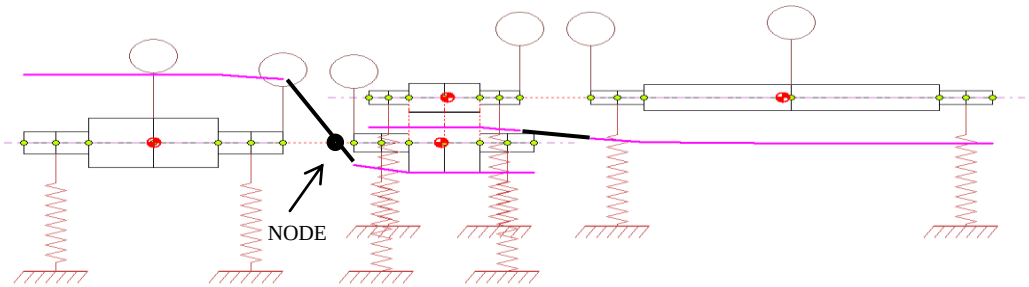

Coupling Stiffness Ratio = 1.0 (Low Speed And High Speed Coupling Stiffnesses Equal)

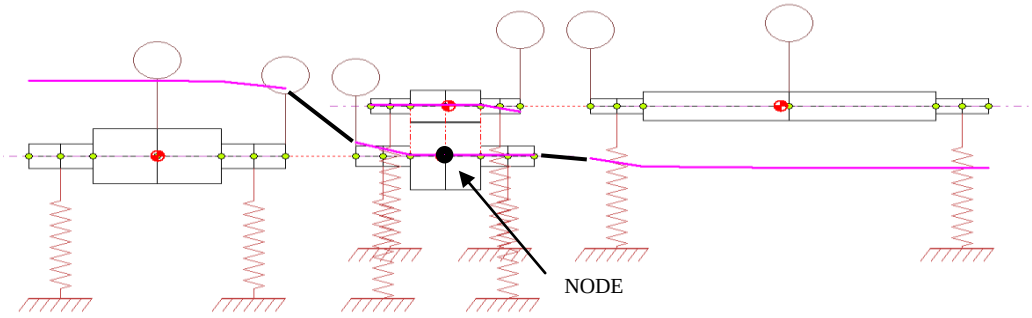

Coupling Stiffness Ratio = 9 (Stiff Low Speed Coupling / Soft High Speed Coupling)

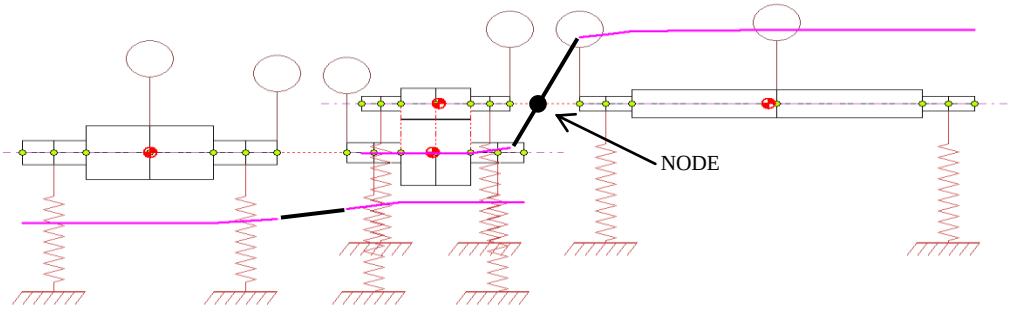

Figure 19 – Torsional Mode Shapes For Various Shaft Stiffness Distributions

CONCLUSIONS

The potentially high shaft torque levels during across-line starts of synchronous motor trains need to be evaluated in the quotation phase to properly size train components to preclude cost overruns and subsequent disruptions in the production schedule. The severity of the resonance condition during a synchronous motor startup is a function of various system parameters. The influence of these system parameters on peak torque levels can be readily evaluated using the closed form solution documented in Appendix 1. This can be effectively used to assess various design options in the pre-quotation phase of a project to obtain the most favorable design based on technical and commercial considerations. The following means have been shown to reduce peak torque levels during startup:

- Decrease pulsating torque at the motor air gap
- Decrease motor terminal voltage
- Reduce startup load
- Increase motor inertia
- Increase system damping through the use of torsionally resilient couplings or torque limiting couplings
- Optimize damping characteristics in the bullgear bearings and to a lesser degree in the pinion bearings as dictated by a coupled torsional-lateral startup analysis
- Adjust the stiffnesses of the low and high speed couplings to position the damping near the optimum value

In the subject example that was evaluated involving a 6 MW compressor train, a thorough investigation of available options was performed that resulted in the most favorable solution based on both technical and commercial considerations. The coupled torsional-lateral analysis was performed which validated the assumed modal damping value of 2.5 percent used in the traditional torsional startup analysis. Optimizing the bearing characteristics in the gearbox has the potential to increase system damping.

The cost evaluation presented in this tutorial applies to the cited example only and is intended to demonstrate the selection process recognizing that other applications may produce different results.

RECOMMENDATIONS

- Since startup load influences component selection and motor design, a process dynamic simulation study should be performed in the quotation phase in instances where it is not possible to sufficiently offload a train during startup.

- Whenever possible, journal bearings in the major train bodies should be sized at least one standard size larger than the shaft ends in the quotation phase in the event it is later discovered that the shaft shear stress or coupling hub slip capacity is later found to be inadequate. Otherwise, if the shaft end diameter needs to be increased, the resulting increase in bearing (and seal) sizes will negatively impact the production schedule.

- API-684 should provide guidelines for coupled torsional-lateral studies for geared systems relative to modeling of gearbox bearings with respect to equivalent bearing load, gear mesh properties, backlash, etc.

- A coupled torsional-lateral analysis should be performed to validate the assumed damping level used in the torsional study for applications that are considered critical or are marginal from a torque transmission or fatigue life standpoint.

REFERENCES

Anwar,I., Colsher, R., 1979, "Computerized Time Transient Torsional Analysis of Power Trains, ASME Paper 79-DET-74.

API 617, 2014, Axial and Centrifugal Compressors and Expander-Compressors for Petroleum, Chemical and Gas Industry Services, Eight Edition, American Petroleum Institute, Washington D.C.

API 684, 2005, API Standard Paragraphs Rotordynamic Tutorial: Lateral Critical Speeds, Unbalance Response, Stability, Train Torsionals, and Rotor Balancing, Second Edition, American Petroleum Institute, Washington D.C.

API 546, 2008, Brushless Synchronous Machines – 500 kVA and Larger, Third Edition, September 2008, American Petroleum Institute, Washington, D.C.

Chen, H.M., McLaughlin, D.W., and Malanowski, S.B., 1983, A Generalized and Simplified Transient Torque Analysis for Synchronous Motor Drive Trains, Proceedings of the Twelfth Turbomachinery Symposium, Turbomachinery Laboratory, Texas A&M University, College Station, Texas, pp 115-119.

Corbo, M.A., Cook, C.P., Yeiser, C.W., and Costello, M.J., 2002, Torsional Vibration Analysis and Testing of Synchronous Motor-Driven Turbomachinery, Proceedings of the Thirty-First Turbomachinery Symposium, Turbomachinery Laboratory, Texas A&M University, Texas, pp. 153-175.

Irvin, T., 1998, Sine Sweep Frequency Parameters, Internet download from tomirvine@aol.com. Used with permission.

Mruk, G., Halloran, J., and Kolodziej, R., 1978, New Method Predicts Startup Torque- Part 1: Analytical Model, Hydrocarbon Processing, pp. 181-186.

Pradetto, J.C., Baumann, U., 2015, Coupled Torsional And Lateral Analysis For The Determination Of The Damping Of The First Torsional Mode Of Synchronous Motor Driven Compressor Trains, Proceedings of the Forty-Fourth Turbomachinery Symposium, Turbomachinery Laboratory, Texas A&M University, Texas.

Yeiser, C.W., Hutten, V., Ayoub, A., and Rheinboldt, R., 2006, Revamping A Gas Compressor Drive Train From 7000 HP To 8000 HP With A New Synchronous Motor Driver And A Controlled Slip Clutch Mechanism, Proceedings of the Thirty-Fifth Turbomachinery Symposium, Turbomachinery Laboratory, Texas A&M University, Texas.

Wright,J., 1975, Large Synchronous Motor Drives: A Review of the Torsional Vibration Problem and It's Solution, Koppers Company, Inc., Baltimore, Maryland.

Wolff, F.H., 1977, Acceleration through Resonance of Multi-Degree of Freedom Systems, the Shock And Vibration Bulletin, Naval Research Laboratory, No. 47, Part 2, pp 127-134.

Appendix 1: Simple Method For Estimating Peak Shaft Torques In Synchronous Motor Trains For Across-Line Starts

The following method can be used to estimate peak shaft torques during across-line starts for trains containing constant speed synchronous motors. It serves as an aid in making decisions relative to the preliminary sizing of couplings and shaft ends. The only information required to use this method are the inertias of the major train components, a motor startup curve, gear ratio, load distribution and the Magnification or 'Q' Factor of the system.

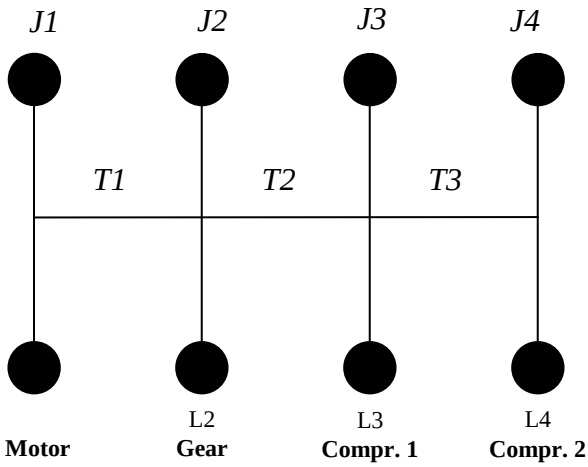

$$T1 = \left(\frac{1}{1}\right) * \left[\{(T_{mean} - T_{load}) * (J2 + J3 + J4) + (L2 + L3 + L4) * T_{load}\} + \{(T_{puls} * Q * \alpha * (J2 + J3 + J4)\}\right]$$

$$T2 = \left(\frac{1}{GR}\right) * \left[\{(T_{mean} - T_{load}) * (J3 + J4) + (L3 + L4) * T_{load}\} + \{(T_{puls} * Q * \beta * (J3 + J4)\}\right]$$

$$T2 = \left(\frac{1}{GR}\right) * \left[\{(T_{mean} - T_{load}) * (J4) + (L4) * T_{load}\} + \{(T_{puls} * Q * \gamma * (J4)\}\right]$$

MEAN TORQUE **ALTERNATING TORQUE**

Definition Of Terms:

J1,J2,J3,J4	Inertia Fraction Of Major Components Referenced To Motor Speed (where J1+J2+J3+J4 = 1.00)
T1, T2, T3	Total Peak Shaft Torque
L2,L3,L4	Load Fraction Of Total Load (where L2+L3+L4 = 1.00)
Tload	Total load *at resonance* from motor startup torque curve
Tmean	Mean motor torque *at resonance* from motor startup torque curve
Tpuls	Pulsating motor torque *at resonance* from motor startup torque curve
α	Mode shape adjustment factor associated with T1 (typically between 0.80 to 1.00)
β	Mode shape adjustment factor associated with T2 (typically between 0.90 to 1.10)
γ	Mode shape adjustment factor associated with T3 (typically between 0.90 to 1.10)
GR	Gear Ratio
Q	Magnification Factor

Notes:

1) All torques are expressed in consistent units such as P.U. or In-Lbs.
2) Gear Ratio (GR) term is applied to both the mean torque and alternating torque, as shown.
3) The inertia values downstream of the gear mesh are referenced to motor speed by multiplying them by the GR squared. The total gear inertia shown on the API 613 data sheets usually reflects this where the Total Gear Inertia = Bullgear Inertia + (Gear Ratio)^2* Pinion Inertia.
4) If the motor speed corresponding to the first torsional natural frequency is not known, the load, mean and pulsating torques can be evaluated at 85 percent rated speed for 60 Hz supply or at 75 percent rated speed for 50 Hz supply.
5) Magnification factors are a function of damping ratio and acceleration rate. See Figure A-1 below.
6) The major bodies need to be arranged as shown below with the motor in the left most position. This method cannot be used for doubled ended motor applications.
7) A complete and thorough transient torsional analysis must be performed once the hardware is selected to confirm torsional acceptability.

Determining Magnification 'Q' Factor

The equations for peak torques shown on the previous page predict the transient response of a torsional system at resonance. The effects of acceleration are taken into consideration by adjusting the magnification 'Q' factor using the method obtained from Wolff (1977) and summarized below.

During transient conditions, $Q = Q(\varepsilon, q)$

Where, Q = Magnification Factor
ε = Damping Ratio
q = Acceleration Factor = $\frac{f_1^2}{h}$ (Hz-sec)
f1 = First Torsional Natural Frequency (Hz)
f_{line} = Electrical Supply Frequency (60 Hz or 50 Hz)
h = Deceleration Rate Of Twice Slip Frequency At Resonance

$$h = \left(\frac{T_{mean} - T_{load}}{TotalTrainInertia}\right) * \left(\frac{2 * f_{line}}{N_{rated}/60}\right) \quad \text{(Hz/Sec)}$$

In this equation, torque is expressed in units of in-lbs. and total train inertia is expressed in units of lbs-in-sec2.

Note that parameter 'h' is the acceleration rate of the twice slip frequency relative to the torsional natural frequency not the acceleration rate of motor speed relative to the torsional natural frequency.

Once 'ξ' and 'q' are determined, the magnification factor 'Q' can be obtained from Figure A-1 below. It is seen from this plot that for rapid acceleration, the damping ratio has less influence on the magnification factor than for the case of slow acceleration. Additionally, for heavily damped systems, the magnification factor is relatively insensitive to acceleration rate.

If the damping ratio is not known, a very conservative estimate for magnification factor can be determined based on a damping ratio of zero. In this instance, the magnification factor 'Q' becomes purely a function of acceleration rate:

During transient conditions, $Q = 3.67 * SQRT\ (q)$ [Special case for zero damping]

At steady state, $Q = \frac{1}{2*\varepsilon}$ [Special case for zero acceleration]

For applications with conventional all-steel couplings, the magnification factor typically ranges from 10 to 20.

Elastomeric couplings (a.k.a Holset or rubber block couplings) are used between the motor and gear to provide higher levels of damping than could otherwise be achieved with all-steel couplings. The published magnification factors for elastomeric couplings range from 3.0 to 4.0 for high damping, SBR, material depending on the material hardness. In the preliminary evaluation, the equivalent magnification factor needs to be estimated based on a weighted average of the relative deflection of the rubber blocks (high damping) and steel elements (low damping). Consequently, the *effective* magnification factor is approximately 1.5x to 2x the published block magnification factor (ie. Qeff = 1.67 x 3.0 = 5.0).

Figure A-1

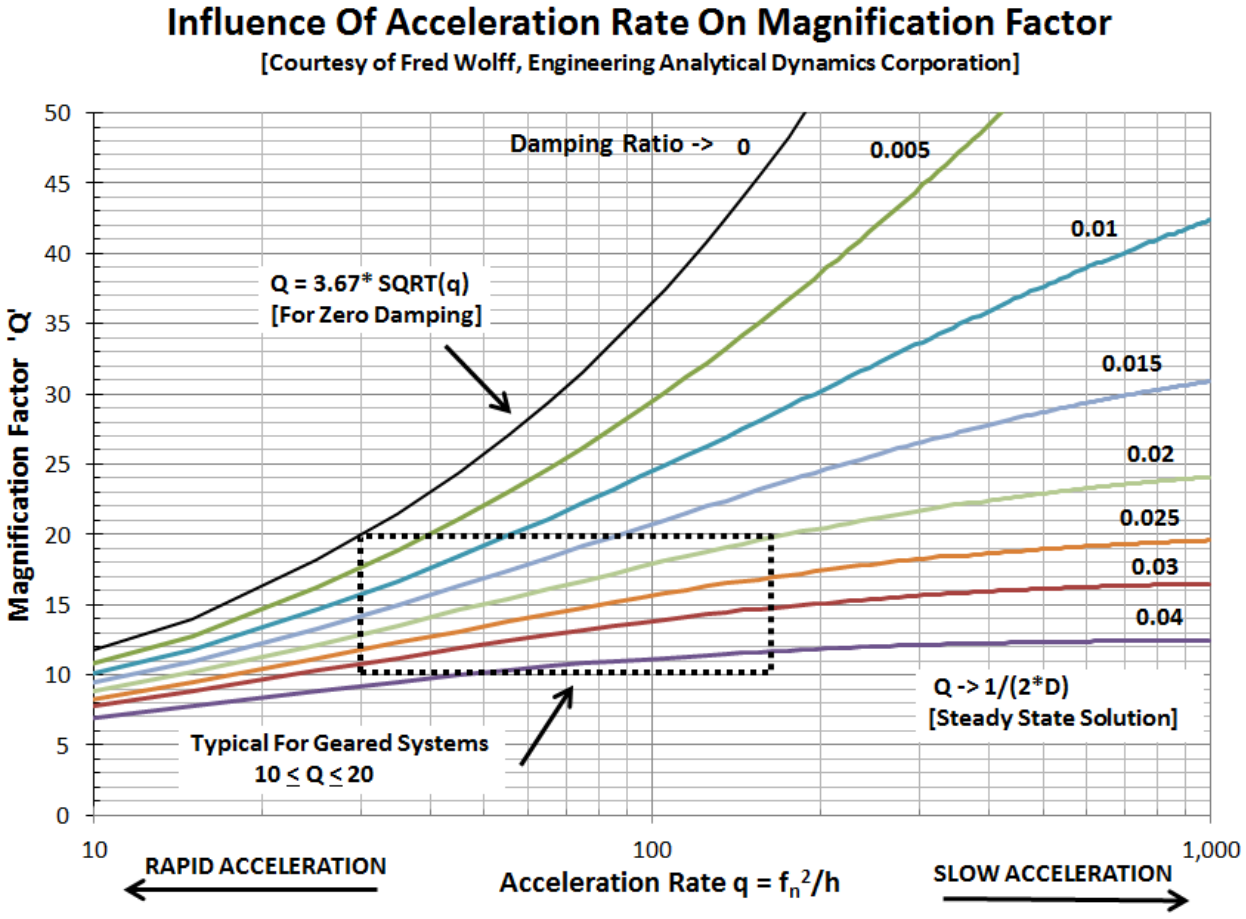

Appendix 2: Application Of Method For The Various Test Cases Evaluated In This Study

BASE OFFERING - AS QUOTED

Tmean=0.98 (typical)
Tpuls= 0.96 (twice normal)
Tload= 0.58 (twice normal)
$\alpha = 0.95$, $\beta = 1.03$
q = 68 Hz-sec
$\xi = 0.025$
Q = 14.3

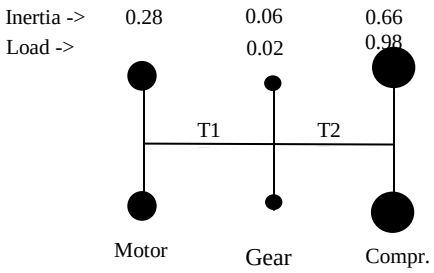

T = [Mean Torque] + [Alternating Torque]

T1 = { [(0.98-0.58) * (0.06+0.66) + (0.02+0.98)*0.58] + 0.96 * 14.3 * 0.95 * (0.06+0.66) }

Load Inertia
Empirical Constant
Magnification Factor
Pulsating Torque

T1 = [0.87] + [9.39] = **10.2 P.U**.

T2 = 1/GR { [0.98-0.58) * (0.66) + (0.98)*0.58] + 0.96 * 14.3 * (1.03) * (0.66) }

Load Inertia
Empirical Constant
Magnification Factor
Pulsating Torque

T2 = [0.83] + [9.33] = **10.2 p.u.**

where 1 p.u. = 1 P.U. / GR is the rated motor torque evaluated down mesh of the gear.

CASE #1: INCREASE COMPONENT SIZES

Effects of Larger Motor & Gear

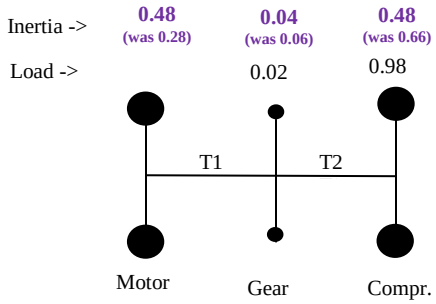

Tmean=0.99 **(was 0.96)**

Tpuls= 0.83 (was 0.98)

Tload= 0.58 (same)

$\alpha = 1.02$, $\beta = 1.02$

q = 59 Hz-sec

$\xi = 0.025$

Q = 14.1 (was 14.3)

T = [Mean Torque] + [Alternating Torque]

T1 = { [(0.99-0.58) * (**0.04+0.48**) + (0.02+0.98)*0.58] + **0.83** * **14.1** * 1.02 * (**0.04+0.48**) }

Load Inertia

Empirical Constant

Magnification Factor

Pulsating Torque

T1 = [0.79] + [6.21] = **7.0 P.U**.

T2 = 1/GR { [0.99-0.58) * (**0.48**) + (0.98)*0.58] + **0.83** * **17.5** * 1.02 * (**0.48**)]

Load Inertia

Empirical Constant

Magnification Factor

Pulsating Torque

T2 = [0.77] + [5.73] = **6.5 p.u.**

CASE #2: ORIGINAL MOTOR WITH TRANSFORMER
(Based on 90 percent Terminal Voltage)

Tmean=0.98* (0.90)^2 = 0.79
Tpuls= 0.96* (0.90)^2 = 0.78
Tload= 0.58
$\alpha = 0.92, \beta = 1.00$
q = 107 Hz-sec (was 68)
$\xi = 0.025$
Q = 16.3 (was 14.3)

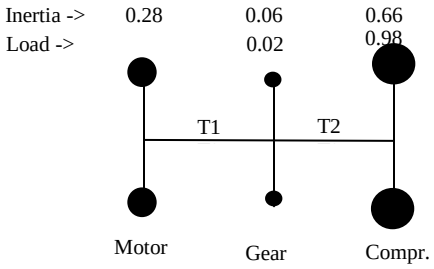

T = [Mean Torque] + [Alternating Torque]

T1 = { [(0.79-0.58) * (0.06+0.66) + (0.02+0.98)*0.58] + 0.78 * 16.3 * 0.92 * (0.06+0.66) }

Load Inertia
Empirical Constant
Magnification Factor
Pulsating Torque

T1 = [0.73] + [8.36] = **9.1 P.U.**

T2 = 1/GR { [0.71-0.58) * (0.66) + (0.98)*0.58] + 0.78 * 16.3 * 1.00 * (0.66)]

Load Inertia
Empirical Constant
Magnification Factor
Pulsating Torque

T2 = [0.71] + [8.38] = **9.1 p.u.**

CASE #3: ELASTOMERIC COUPLING

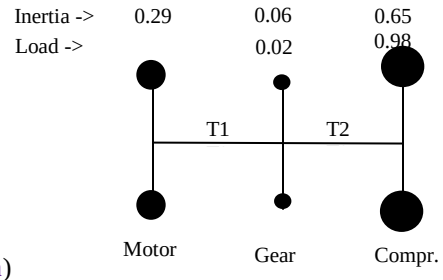

Tmean=0.99
Tpuls= 0.97
Tload= 0.58
α = 1.02, β = 1.10
q = 39 Hz-sec
ξ =0.098 (for 70 durometer block material)
Q = 5.1 (effective damping including shaft deflection)

T = [Mean Torque] + [Alternating Torque]

T1 = { [(0.99-0.58) * (0.06+0.65) + (0.02+0.98)*0.58] + 0.97 * 5.1 * 1.02 * (0.06+0.65) }

Load Inertia
Empirical Constant
Magnification Factor
Pulsating Torque

T1 = [0.87] + [3.58] = **4.5 P.U.**

T2 = 1/GR { [0.99-0.58) * **(0.65)** + (0.98)*0.58] + 0.97 * 5.1 * 1.10 * (**0.65**) }

Load Inertia
Empirical Constant
Magnification Factor
Pulsating Torque

T2 = [0.84] + [3.53] = **4.4 p.u.**

CASE #4: GRID STYLE COUPLING

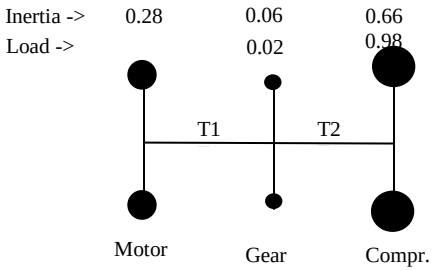

Tmean=0.98
Tpuls= 0.97
Tload= 0.58
α = 0.88, β = 1.04
q = 68 Hz-sec
ξ =0.055
Q = 9.0

T = [Mean Torque] + [Alternating Torque]

T1 = { [(0.99-0.58) * (**0.06+0.66**) + (0.02+0.98)*0.58] + 0.97 * **9.0** * 0.88 * (**0.06+0.66**) }

Load Inertia
Empirical Constant
Magnification Factor
Pulsating Torque

T1 = [0.88] + [5.53] = **6.4 P.U.**

T2 = 1/GR { [0.99-0.58) * (**0.66**) + (0.98)*0.58] + 0.97 * **9.0** * 1.04 * (**0.66**)]

Load Inertia
Empirical Constant
Magnification Factor
Pulsating Torque

T2 = [0.84] + [5.99] = **6.8 p.u.**

CASE #5: SLIP CLUTCH COUPLING

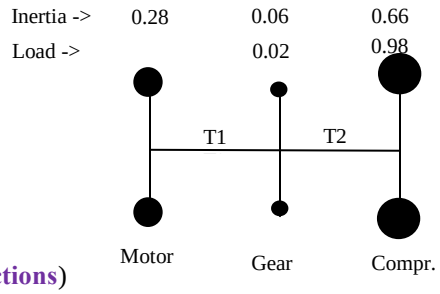

Tmean=0.98
Tpuls= 0.96
Tload= 0.58
α = 0.96, β = 0.98
q = 68 Hz-sec
ξ = N/A
Q = 4.4 (Back calculated from manufacturer's predictions)

T = [Mean Torque] + [Alternating Torque]

T1 = { [(0.99-0.58) * (0.06+0.66) + (0.02+0.98)*0.58] + 0.96 * 4.4 * 0.96 * (0.06+0.66) }

Load Inertia
Empirical Constant
Magnification Factor
Pulsating Torque

T1 = [0.87] + [2.92] = **3.8 P.U.**

T2 = 1/GR { [0.99-0.58) * (0.66) + (0.98)*0.58] + 0.96 * 4.4 * (0.98) * (0.66)]

Load Inertia
Empirical Constant
Magnification Factor
Pulsating Torque

T2 = [0.84] + [2.73] = **3.6 p.u.**

CASE #6: VISCOUS ROTATIONAL DAMPER

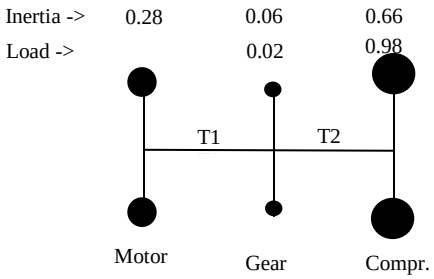

Tmean=0.98
Tpuls= 0.96
Tload= 0.58
α = 0.95, β = 0.97
q = 68 Hz-sec
ξ =0.15
Q = 3.3 (effecting damping including shaft deflection)

T = [Mean Torque] + [Alternating Torque]

T1 = { [(0.98-0.58) * (0.06+0.66) + (0.02+0.98)*0.58] + 0.97 * 3.3 * 0.95 * (0.06+0.66) }

Load Inertia
Empirical Constant
Magnification Factor
Pulsating Torque

T1 = [0.87] + [2.19] = **3.1 P.U**.

T2 = 1/GR { [0.98-0.58) * (0.66) + (0.98)*0.58] + 0.97 * 3.3 * (0.97) * (0.66)]

Load Inertia
Empirical Constant
Magnification Factor
Pulsating Torque

T2 = [0.83] + [2.05] = **2.9 p.u.**

CASE #7: HYDRAULIC CLUTCH PRECEEDING GEAR
(Assume no hydraulic fluid is in coupling during startup)

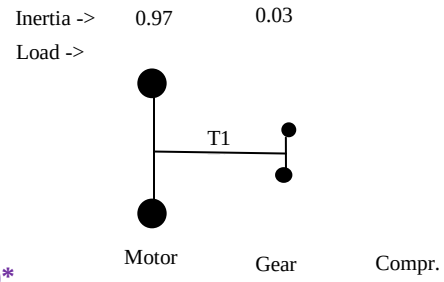

Tmean=0.96
Tpuls= 0.73
Tload= 0
α = 1.0, β = N.A.
q = 30 Hz-sec
ξ =0.01
Q = 16 (effecting damping including shaft deflection)*

T = [Mean Torque] + [Alternating Torque]

T1 = { [(0.96-0) * (**0.03**) + (0) + 0.73 * **16** * 1.0 * (**0.03**) }

Load Inertia
Empirical Constant
Magnification Factor
Pulsating Torque

T1 = [0.03] + [0.35] = **0.4 P.U.**

T2 = 0

* It is assumed that the 1st torsional natural frequency is far removed from electrical supply frequency

CASE #8: PONY MOTOR + HYDRAULIC CLUTCH

No startup transients to consider.

CASE #9: VFD Starter

No startup transients exist relative to the twice slip motor frequency. Integer and non-integer multiples of electrical frequency need to be evaluated from a life cycle fatigue standpoint but the pulsating torque ripple associated with waveform distortion is an order of magnitude less than the twice slip component of synchronous motors started across-line so it has less impact on component selection.

CASE #10: REDUCED COMPRESSOR LOAD *

Tmean=0.96 (was 0.98)
Tpuls= 0.63 (was 0.96)
Tload= 0.29 (was 0.58)
$\alpha = 0.96, \beta = 1.05$
q = 36 Hz-sec
$\xi = 0.025$
Q = 12.5

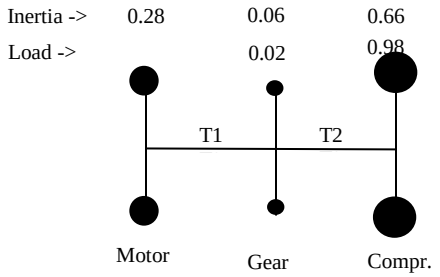

T = [Mean Torque] + [Alternating Torque]

T1 = { [(0.96-0.29) * (0.16+0.47) + (0.02+0.98)*0.58] + 0.63 * 12.5 * 0.96 * (0.06+0.66) }

Load Inertia
Empirical Constant
Magnification Factor
Pulsating Torque

T1 = [0.79] + [5.44] = **6.2 P.U.**

T2 = 1/GR { [0.96-0.29) * (0.47) + (0.98)*0.58] + 0.63 * 12.5 * (1.05) * (0.66)]

Load Inertia
Empirical Constant
Magnification Factor
Pulsating Torque

T2 = [0.74] + [5.46] = **6.2 p.u.**

* Hypothetical case where pulsating torque is reduced by 33 percent and 0.40 PU load assumed at rated speed and where torque varies with the square of the speed.

CASE #11: CUSTOMIZED MOTOR - FINAL DESIGN*

Tmean=0.96 (was 0.98)
Tpuls= 0.65 (was 0.96)
Tload= 0.57
$\alpha = 0.85, \beta = 1.10$
q = 86 Hz-sec
$\xi = 0.025$
Q = 15.3

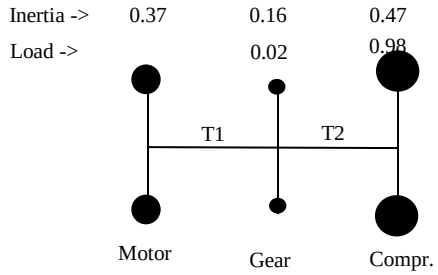

T = [Mean Torque] + [Alternating Torque]

T1 = { [(0.96-0.58) * (0.16+0.47) + (0.02+0.98)*0.58] + 0.65 * 15.3 * 0.85 * (0.16+0.47) }

Load Inertia
Empirical Constant
Magnification Factor
Pulsating Torque

T1 = [0.82] + [5.32] = **6.1 P.U.**

T2 = 1/GR { [0.96-0.58) * (0.47) + (0.98)*0.58] + 0.65 * 15.3 * (1.10) * (0.47)]

Load Inertia
Empirical Constant
Magnification Factor
Pulsating Torque

T2 = [0.75] + [5.14] = **5.9 p.u.**

Note: This initial calculation was based on infinite bus characteristics whereas the final calculation used in the final report was based on an estimated 5 percent initial voltage dip in the electrical supply with a 2 percent voltage recovery at resonance.

Appendix 3: Alternate Method For Estimating Peak Shaft Torques In Synchronous Motor Trains For Across-Line Starts
(Courtesy of Fred Wolff, Engineering Analytical Dynamics Corporation)

To estimate the maximum alternating component of shaft response from a forced-vibration analysis, consider the following general equation of motion for a torsional model:

$$[I]\{\ddot{\theta}\}+[C]\{\dot{\theta}\}+[K]\{\theta\}=\{T_{exc}\}$$

where $[I]$ is a diagonal inertia matrix, $[C]=\alpha[I]+\beta[K]$ is a proportional damping matrix, $[K]$ is the stiffness matrix, $\{T_{exc}\}$ is input excitation torque vector, $\{\ddot{\theta}\}$, $\{\dot{\theta}\}$, and $\{\theta\}$ are the angular acceleration, velocity, and displacement vectors, respectively.

Apply a normal mode transformation $\{\theta\}=[P]\{q\}$ to equation of motion then multiply through by the transpose of modal matrix gives the uncoupled equations of motion in terms of modal coordinates, q.

$$[P]^T[I][P]\{\ddot{q}\}+[P]^T[\alpha[I]+\beta[K]][P]\{\dot{q}\}+[P]^T[K][P]\{q\}=[P]^T\{T_{exc}\}$$

or

$$[Ig]\{\ddot{q}\}+[Cg]\{\dot{q}\}+[Kg]\{q\}=\{Tg\}$$

where the generalized inertia matrix $[Ig]$ is a diagonal matrix of terms $Ig_n=\sum_j I_j P_{j,n}^2$, the generalized damping matrix $[Cg]$ is a diagonal matrix of terms $Cg_n=\alpha Ig_n+\beta Kg_n$, the generalized stiffness matrix $[Kg]$ is a diagonal matrix of terms $Kg_n=\omega_n^2 Ig_n$ and the generalized torque vector $\{Tg\}$ is torque vector whose components $Tg_n=\sum_j P_{j,n} Texc_j$ represents the amount of torque excitation for each mode.

For any mode n, the second order differential equation of motion can be written as

$$Ig_n\ddot{q}_n+Cg_n\dot{q}_n+Kg_nq_n=Tg_nT_{exc}\sin\omega t$$

The solution to the above equation of motion has two parts: a complementary solution which is the solution to the homogeneous equation giving the damped free vibration and a particular solution which is the steady state solution or the forced-vibration response to harmonic motion at frequency ω.

For the particular solution assume

$$q_n(t)=q_n\mathrm{Sin}(\omega t-\phi)$$

Substituting into differential equation gives

$$\left[-\omega^2 Ig_n\right]q_n\mathrm{Sin}(\omega t-\phi)+\omega Cg_nq_n\mathrm{Cos}(\omega t-\phi)+Kg_n\mathrm{Sin}(\omega t-\phi)=Tg_nT_{exc}\mathrm{Sin}\omega t$$

Expanding equation gives

$$-\omega^2 Ig_n q_n [Sin\omega t Cos\phi - Sin\phi Cos\omega t] + \omega Cg_n [Cos\omega t Cos\phi + Sin\omega t Sin\phi] +$$
$$Kg_n [Sin\omega t Cos\phi - Sin\phi Cos\omega t] = Tg_n T_{exc} Sin\omega t$$

Collecting like terms gives for the coefficient of the $Sin\omega t$ terms

$$[Kg_n - \omega^2 Ig_n] q_n Cos\phi + [\omega Cg_n] q_n Sin\phi = Tg_n T_{exc}$$

Using the identity

$$Cos(\omega t - \phi) = Cos\omega t Cos\phi + Sin\omega t Sin\phi$$

Gives for the solution

$$q_n(t) = \frac{1}{\sqrt{[Kg_n - \omega^2 Ig_n]^2 + [\omega Cg_n]^2}} Tg_n T_{exc} Sin(\omega t - \phi)$$

where

$$\frac{Sin\phi}{Cos\phi} = \frac{\omega Cg_n}{[Kg_n - \omega^2 Ig_n]} \quad \text{or} \quad \phi = \tan^{-1}\left\{\frac{\omega Cg_n}{Kg_n - \omega^2 Ig_n}\right\}$$

The peak response is

$$q_n(max) = \frac{Tg_n}{\sqrt{[Kg_n - \omega^2 Ig_n]^2 + [\omega Cg_n]^2}} T_{exc}$$

Divide numerator and denominator by Kg_n gives

$$q_n(max) = \frac{Tg_n / Kg_n}{\sqrt{\left[1 - \left(\omega / \omega_n\right)^2\right]^2 + \left[2\xi_n \omega / \omega_n\right]^2}}$$

Where the phase angle is

$$\phi = \tan^{-1} \frac{2\xi_n \, \omega / \omega_n}{1 - \left(\omega / \omega_n \right)^2}$$

Since the magnification Q_n can be defined as

$$Q_n = \frac{1}{\sqrt{\left[1 - \left(\omega / \omega_n \right)^2 \right]^2 + \left[2\xi_n \, \omega / \omega_n \right]^2}}$$

The modal response is given as

$$q_n(t) = Q_n \frac{Tg_n}{Kg_n} T_{exc} \sin(\omega t - \phi)$$

Since the displacement at node (i) in mode n is $\theta_{i,n} = P_{i,n} q_n$ the torque across the shaft between node I and node i+1 can be written as

$$T_n(i,i+1) = T_{i,n} - T_{i+1,n} = K(i,i+1)\{\theta_{i,n} - \theta_{i+1,n}\} = K(i,i+1)\{P_{i,n} - P_{i+1,n}\} q_n$$

Using the above definition for the peak modal response, the peak torque response across shaft 1, 1+1 can be expressed as

$$T_n(i,i+1) = Q_n \left| P_{i,n} - P_{i+1,n} \right| \frac{K(i,i+1)}{Kg_n} Tg_n T_{exc}$$

The ratio between the peak shaft torque across shaft I, i+1 in mode n is written as

$$\frac{T_n(i,i+1)}{T_{exc}} = Q_n \left| P_{i,n} - P_{i+1,n} \right| \frac{K(i,i+1)}{Kg_n} Tg_n$$